Development of Selenium-75 as a Brachytherapy Source

Jake Reid



Medical Physics Unit McGill University Montréal, Québec, Canada

August 15, 2023

A thesis submitted to McGill University in partial fulfillment of the requirements of the degree of Master of Science in medical radiation physics.

© Jake Reid 2023

Abstract

High-dose-rate (HDR) brachytherapy is a well-established and effective radiation treatment modality utilized in the management of various cancers. It involves the temporary placement of a sealed highly radioactive photon emitting source (a seed), usually ¹⁹²Ir, inside or near the tumor to deliver therapeutic doses of radiation. Image-guided HDR brachytherapy provides an optimal dose distribution in the tumour with decreased toxicity to organs at risk due to the steep dose gradient from brachytherapy sources. However, dose distribution from brachytherapy sources is identical in all directions, which often results in less-than-ideal tumour dose conformity leading to dose spillage to healthy tissues causing side effects.

To mitigate this issue, novel shielding techniques have been developed. Shields should be capable of significantly reducing the radiation source's intensity, ideally by several half-value layers. Furthermore, they must be compact enough to be utilized in brachytherapy applicators and catheters. While achieving this is feasible for intracavitary HDR brachytherapy, it becomes challenging for interstitial HDR brachytherapy due to the high energy of ¹⁹²Ir and small diameters of the catheters. Consequently, it becomes necessary to explore alternative lower-energy radiation sources. This thesis pursued two main objectives. Firstly, it aimed to design, manufacture and characterize a lower energy

Abstract

brachytherapy source, specifically ⁷⁵Se, to investigate its physical and dosimetric properties. The goal was to improve brachytherapy treatments by reducing the absorbed dose to surrounding healthy tissues while achieving acceptable treatment times and dose homogeneity. Secondly, treatment plans were simulated using the Monte Carlo method on data from a rectal cancer patient to further validate the benefits of utilizing ⁷⁵Se as a brachytherapy source. These simulations were conducted using a rectal static shield as well as a dynamically rotating shield. This allowed for a comparison of treatment metrics between ⁷⁵Se and the commonly used ¹⁹²Ir, providing valuable insights into the potential advantages of ⁷⁵Se in brachytherapy applications.

The manufacturing process of the ⁷⁵Se source involved encapsulating a vanadium diselenide compound in titanium. The source was irradiated at the McMaster Nuclear Reactor. Thorough evaluations were carried out, involving a range of assessments. These included visual inspections to identify deformations, activity measurements, analysis of radiation contaminants, and a gamma index analysis that compared film measurements with Monte Carlo simulated results. Furthermore, Monte Carlo simulations were employed to investigate the differences in shield effectiveness between the use of ⁷⁵Se and ¹⁹²Ir. To characterize the source, Monte Carlo simulations using the standardized formalism of TG-43 were completed.

The manufacturing of a low activity 75 Se brachytherapy source was achieved successfully, demonstrating no deformations. The radiation contaminants produced by the titanium and vanadium in the source were below 1% of the overall contribution of the 75 Se brachytherapy source. Notably, the 75 Se brachytherapy source enabled remarkable shielding effectiveness. When using 75 Se with the rectal static shield and dynamically rotating shield, the shields were able to attenuate the dose 4.86 ± 0.12 and 5.41 ± 0.12

Abstract

times better than when using 192 Ir, respectively. This improvement in shielding effectiveness allowed for better optimized treatment plans to be achieved when using 75 Se. The treatment time and dose homogeneity index were similar to the ones achieved with 192 Ir and all dosimetric indices to organs at risk were improved. Most notably, the D_{2cc} to the contralateral rectum was reduced by 0.97 Gy and the D_{50} of the rectum was reduced by 1.17 Gy. These results display the potential that 75 Se has on the significant improvement of brachytherapy treatments and serves as the initial steps to bringing this source to clinical implementation.

Abrégé

La curiethérapie est une modalité de traitement par rayonnement bien établie et efficace pour divers cancers. Elle implique le placement d'une source hautement radioactive émettant des photons (une graine), généralement l'¹⁹²Ir, dans ou près de la tumeur pour délivrer des doses thérapeutiques de rayonnement. La curiethérapie à haute dose guidée par imagerie offre une distribution optimale de la dose dans la tumeur avec une toxicité réduite pour les organes à risque grâce au fort gradient de dose des sources de curiethérapie. Cependant, la distribution de dose des sources de curiethérapie est identique dans toutes les directions, ce qui conduit souvent à une dose tumorale moins conforme et à des effets secondaires dus à l'irradiation de tissus sains.

Pour atténuer ce problème, de nouvelles techniques de blindage ont été développées. Les blindages doivent réduire significativement l'intensité de la source de rayonnement, idéalement par plusieurs couches à demi-épaisseur. De plus, ils doivent être suffisamment compacts pour être utilisés dans les applicateurs de curiethérapie. Bien que cela soit possible pour la curiethérapie HDR intracavitaire, cela devient difficile pour la curiethérapie HDR interstitielle en raison de la haute énergie de l'¹⁹²Ir et des petits diamètres des cathéters. Par conséquent, il est nécessaire d'explorer des sources de rayonnement à plus basse énergie. Cette thèse avait deux objectifs principaux.

Abrégé v

Premièrement, concevoir, fabriquer et caractériser une source de curiethérapie à basse énergie, le ⁷⁵Se, pour étudier ses propriétés physiques et dosimétriques. L'objectif était d'améliorer les traitements de curiethérapie et d'en augmenter l'efficacité. Deuxièmement, simuler des plans de traitement à l'aide de la méthode de Monte Carlo sur les données d'un patient atteint de cancer du rectum pour valider davantage les avantages de l'utilisation du ⁷⁵Se comme source de curiethérapie. Cela a permis de comparer les traitements entre le ⁷⁵Se et l'¹⁹²Ir, fournissant ainsi des informations précieuses sur les avantages potentiels du ⁷⁵Se en curiethérapie.

Le processus de fabrication de la source de ⁷⁵Se impliquait l'encapsulation d'un composé de diséléniure de vanadium dans du titane. La source a été irradiée au Réacteur Nucléaire de McMaster. Des évaluations approfondies ont été menées, comprenant des inspections visuelles pour identifier les déformations, des mesures d'activité, l'analyse des contaminants radioactifs et une analyse de l'indice gamma comparant les mesures aux résultats simulés par Monte Carlo. De plus, des simulations Monte Carlo ont été utilisées pour étudier les différences d'efficacité de blindage entre le ⁷⁵Se et l'¹⁹²Ir. Pour caractériser la source, des simulations Monte Carlo utilisant le formalisme normalisé TG-43 ont été réalisées.

La fabrication d'une source de curiethérapie au 75 Se à faible activité a été réalisée avec succès, démontrant l'absence de déformations. Les contaminants radioactifs produits par le titane et le vanadium dans la source étaient inférieurs à 1% de la contribution totale de la source de curiethérapie au 75 Se. Notamment, la source de curiethérapie au 75 Se a permis une efficacité de blindage remarquable. Lors de l'utilisation du 75 Se avec le blindage statique rectal et le blindage rotatif dynamique, les blindages ont pu atténuer la dose 4.86 \pm 0.12 et 5.41 \pm 0.12 fois mieux que lors de l'utilisation de l' 192 Ir, respectivement. Cette

Abrégé vi

amélioration de l'efficacité de blindage a permis d'obtenir de meilleurs plans de traitement optimisés avec le 75 Se. Notamment, le D_{2cc} pour le rectum controlatéral et le ballon utilisé pour le positionnement ont été réduits de 0.97 et 2.05 Gy respectivement, et le D_{50} du rectum a été réduit de 1.17 Gy. Ces résultats montrent le potentiel du 75 Se pour améliorer considérablement les traitements de curiethérapie et ouvrent la voie à une mise en œuvre clinique future.

Acknowledgements

I want to express my sincere gratitude to Dr. Shirin A. Enger for her invaluable support and guidance throughout this work. Her supervision and encouragement have been instrumental in pushing me to challenge myself and achieve goals that I never thought possible. I would also like to acknowledge Jonathan Kalinowski for his tremendous help and support during my master's program, both in coursework and in the completion of this project. His unwavering assistance and emotional support have been crucial in meeting the high standards set for this work.

I extend my thanks to Dr. John Munro III for generously sharing his expertise in source manufacturing and for his active participation in productive meetings, even after his retirement. I am grateful to Dr. Andrea Armstrong for her extensive knowledge in nuclear reactors and radioisotopes. Additionally, I want to express my appreciation for her warm hospitality and excellent guidance during the visit to McMaster Nuclear Reactor. I am particularly grateful to Dr. Hamed Bekerat for his assistance and guidance in conducting film measurements. I deeply appreciate his dedication, especially when he stayed late at work on a Friday to complete time-sensitive scans. I would also like to acknowledge Kelly Wright and Dr. Morim for their enthusiastic support during the measurements conducted at McMaster Nuclear Reactor.

Completing this master's program during the challenging times of the COVID-19 pandemic while adapting to a new city would not have been possible without the tremendous support from my family and friends. I want to express my heartfelt thanks to Hailey, Jonathan, Shogo, and Cristian, my fellow cohort members, for creating an outstanding working environment during our classes. I am grateful to my lab neighbor, Sebastien, for his continuous support and motivation both inside and outside of work. To everyone in the Enger lab, thank you for creating such an open and welcoming work environment that has made Montreal a place I will always cherish. Lastly, I would like to acknowledge the unwavering support and foundation provided by my phenomenal parents and oma. Their love and encouragement have been vital in my journey.

Contribution of Authors

This thesis presents two manuscripts to be submitted for publication Chapter 2: Manufacturing of a Selenium-75 brachytherapy source and Chapter 3: Dosimetric Analysis of a Selenium-75 Brachytherapy Source.

As the first author on these manuscripts, I designed and assessed the performance of the prototype selenium-75 brachytherapy source. The contributions of the co-authors are as follows:

- Jonathan Kalinowski: Completed the Monte Carlo simulations for the TG-43
 parameters as well as the film measurements, completed the preliminary analysis of
 the film simulations, aided in the measurements completed at McMaster Nuclear
 Reactor and provided valuable feedback on the manuscripts.
- Dr. John Munro III: Shared his expertise in source manufacturing.
- Dr. Hamed Bekerat: Shared his expertise in dosimetry measurements and helped with the design of the measurement setups as well as the scans of all films.
- Dr. Andrea Armstrong: Shared her expertise in nuclear reactor isotope production, completed the analysis of the gamma spectroscopy data and helped with completing all measurements at McMaster Nuclear Reactor.

• Dr. Shirin A Enger: Provided guidance and insights throughout the development of the prototype brachytherapy source and valuable feedback on the manuscripts.

This work was presented at the following conferences:

- Jake Reid, Jonathan Kalinowski, John Munro III, Hamed Bekerat, Andrea Armstrong, Shirin A Enger. 'Investigation of the feasibility of selenium-75 as a viable brachytherapy source'. ESTRO. Vienna, May 12-16, 2023 (Oral)
- Jake Reid, Jonathan Kalinowski, John Munro III, Hamed Bekerat, Andrea Armstrong, Shirin A Enger. 'Development of a Selenium-75 Brachytherapy Source'. International Conference on Isotopes. Saskatoon, July 23-27, 2023 (Oral).

This work will be presented at the following conferences:

 Jake Reid, Jonathan Kalinowski, John Munro III, Hamed Bekerat, Andrea Armstrong, Shirin A Enger. 'Is Selenium-75 a Feasible HDR Brachytherapy Source?'. CARO-COMP Joint Scientific Meeting. Montreal, September 20-23, 2023 (Oral).

Contents

1 Introduction			1
	1.1	Preface	1
	1.2	Objectives	2
2	Bac	ekground and Literature Review	4
	2.1	Brachytherapy	4
		2.1.1 Dose Rate	5
		2.1.2 Dosimetry	5
	2.2	Model-based Dose Calculation	10
	2.3	Intensity Modulated Brachytherapy	11
		2.3.1 High Dose Rate Endorectal Brachytherapy	14
	2.4	Desirable Characteristics of Brachytherapy Sources	16
		2.4.1 Selenium-75	18
	2.5	Radiochromic Film	19
3	Mai	nufacturing of a Selenium-75 brachytherapy source	20
	9 1	Abatuact	ດ1

xii

	3.2	Introd	uction	22
		3.2.1	Brachytherapy	22
		3.2.2	Selenium-75	24
		3.2.3	Objectives	26
	3.3	Materi	ials and Methods	26
		3.3.1	Source Design and Characterization	27
		3.3.2	Source Manufacturing	28
		3.3.3	Film Measurements	30
	3.4	Result	S	34
		3.4.1	TG-43U1 Parameters	34
		3.4.2	Source Characteristics	34
		3.4.3	Film	38
	3.5	Discus	sion	39
		3.5.1	TG-43 Calculations	41
		3.5.2	Physical Properties	43
		3.5.3	Film Measurements	44
	3.6	Conclu	usion	46
	3.7	Appen	ndix A	47
	3.8	Appen	ndix B	47
4	Brio	lging t	text	49
5	Dos	imetri	c Analysis of a Selenium-75 Brachytherapy Source	51
	5.1	Abstra	act	52
	5.2	Introd	uction	54

6	D:	cussion		77
	5.9		ndix C	
	5.8	Apper	ndix B	75
	5.7	Apper	ndix A	74
	5.6	Concl	usion	74
	5.5	Discus	ssion	69
		5.4.2	Simulations in Patient	66
		5.4.1	Simulations in Water	64
	5.4	Result	ts	64
		5.3.1	Monte Carlo Simulations	60
	5.3	Mater	ials and Methods	60
		5.2.4	Selenium-75	58
		5.2.3	Brachytherapy Sources	57
		5.2.2	Intensity Modulated Brachytherapy	56
		5.2.1	High Dose Rate Brachytherapy	54

List of Figures

2.1	Brachytherapy dosimetry coordinate system	7
2.2	Radial Dose functions of five different radiation sources	9
2.3	Cross-sectional view of cylindrical intracavitary mold applicator (left) with	
	the full assembly (right)	15
3.1	Geometric design of the $^{75}\mathrm{Se}$ theoretical source with dimensions given in	
	millimeter	28
3.2	Measurement setup for film measurements. Solid water phantom is located	
	behind lead bricks for radiation safety. The films were placed and centered on	
	each slab.	31
3.3	TG-43 parameter comparison between $^{75}\mathrm{Se}$ and $^{192}\mathrm{Ir}$ sources for a) the radial	
	dose function and b) the 2D anisotropy function	35
3.4	Dosimetric comparison plots for the -1 cm source to film distance between the	
	Monte Carlo (top left) and physical film (top right) dose distributions. The	
	absolute dose difference (bottom left) and gamma values (bottom right) are	
	shown. The dwell time was set to 72000 s	38
5 1	Source dimensions of the colonium source	61

5.2	The axial dose distributions in water for both shields are used to calculate the	
	transmission factors. a) and b) are the comparison of the rigid 180° IMBT	
	shield for both sources, and c) and d) are the comparison of the ICMA static	
	shield for both sources	65
5.3	Sagittal dose distributions after final MC simulation in a heterogeneous	
	patient phantom using the IMBT shield for the $^{192}\mathrm{Ir}$ source (left) and $^{75}\mathrm{Se}$	
	source (right). The contours displayed are the structures used to optimize	
	the plan, and in the slices, the position of the applicator can be seen	67
5.4	Axial dose distributions after final MC simulation in a heterogeneous patient	
	phantom using the ICMA static shield for the $^{192}\mathrm{Ir}$ source (left) and $^{75}\mathrm{Se}$	
	source (right). The contours displayed are the structures used to optimize the	
	plan	67
5.5	Intracavitary mold applicator used conventionally in HDR brachytherapy	
	rectal treatments. Central lumen capable of holding an 8 mm tungsten shield.	74
5.6	Rigid 180° IMBT shield designed by Thibodeau-Antonacci $et\ al.$ The diameter	
	of the shield is 15 mm with 7.5 mm of tungsten shielding. The light grey part	
	is a removable silicone rubber to enclose the central lumen	74

List of Tables

3.1	Radioactive impurities in titanium wire piece that weighed 0.0168 g. The	
	table also contains extrapolation information for impurities per mg of sample.	
	Very short-lived radionuclides will not appear in this spectrum due to the	
	delay between end of bombardment and gamma spectrum acquisition	36
3.2	Radioactive impurities in Vanadium pieces that weighed $0.2154~\mathrm{g}$. The table	
	also contains extrapolation information for impurities per mg of sample. Very	
	short-lived radionuclides will not appear in this spectrum due to the delay	
	between EoB and gamma spectrum acquisition	37
3.3	Film results achieved using a source activity correction factor of 1.237. $$	39
5.1	Transmission factors for both the conventional HDR brachytherapy shield and	
	the rigid 180° IMBT shield	66
5.2	Plan metrics for both $^{75}\mathrm{Se}$ and $^{192}\mathrm{Ir}$ treatment plans using the IMBT shield.	
	The Type A uncertainty for both plans was $<1\%$ on the 100% isodose line .	69

Chapter 1

Introduction

1.1 Preface

High dose rate (HDR) brachytherapy is a radiotherapy treatment modality that involves the insertion of a radioisotope inside or near the tumour to deliver prescribed doses of radiation. This treatment modality allows for more localized and higher doses of radiation to tumours compared to other modalities such as external beam radiotherapy. Although HDR brachytherapy has these advantages, it has the limitation that the dose emitted by the radioisotope is isotropically distributed. This restricts the escalation of dose to the tumour as surrounding healthy tissues will receive higher doses with higher prescribed radiation doses. To mitigate this risk, the use of metallic shields have been investigated and implemented clinically to modulate the intensity of the radiation dose during brachytherapy treatments. These techniques have shown great improvements in reducing dose received by healthy tissue in brachytherapy treatments, which has be proven by clinical and theoretical findings.

Despite this improvement in brachytherapy treatments, the effectiveness of these

1. Introduction 2

shields in the attenuation of dose produced by radioisotopes is impeded by the physical constraints imposed by the size of the applicators and catheters used in treatments. With these small shield thicknesses, the dose produced by the most commonly used high energy brachytherapy source, ¹⁹²Ir, does not get attenuated by several half value layers. This restricts brachytherapy treatments with the use of shields to not reach its full potential.

Recognizing the potential of these shielding techniques, it was decided to investigate potential alternative brachytherapy sources. Compared to ¹⁹²Ir, this alternative source should have lower gamma energies to allow for better shielding attenuation, have a longer half-life, be capable of completing similar treatment times and be comparable in production price. Through our research, ⁷⁵Se showed promise in achieving all these characteristics. Therefore, this thesis investigated the benefits of ⁷⁵Se as well as the feasibility of developing a ⁷⁵Se brachytherapy source for use in brachytherapy applications with novel shielding techniques.

1.2 Objectives

This work aimed to further improve brachytherapy treatments by designing, manufacturing and testing a novel ⁷⁵Se brachytherapy source. This source can lead to more conformal dose distributions, reducing the dose in treatments to healthy tissue. The first goal was to design and manufacture the source assessing the radiation output by measuring the dosimetric properties of the source using radiochromic film as well as completing a spectral analysis to analyze contaminants. The second goal was to assess the potential benefits of using the ⁷⁵Se source compared to the presently used ¹⁹²Ir source for both IMBT and presently used static shield design treatment plans for rectal cancer treatment.

1. Introduction 3

The radiation attenuation capacity of these shields was compared, and treatment plans were optimized using a Monte Carlo-based treatment planning software. For the treatment plans, the absorbed dose to the tumour and surrounding organs at risk were calculated and compared to quantify the results.

Chapter 2

Background and Literature Review

2.1 Brachytherapy

High dose rate (HDR) brachytherapy is a form of radiotherapy that involves temporarily placing a sealed photon-emitting radioactive source, usually ¹⁹²Ir, inside or near the tumour irradiating from the inside out, in contrast with external beam radiotherapy that irradiates cancer from the outside. Brachytherapy can be used as a monotherapy or combined with other treatment modalities for the treatment of localized and small tumours [1]. The technique involves directing radioactive sources to the tumor site through various approaches, including intracavitary, interstitial, intraluminal, surface (mould), intraoperative, and intravascular methods. The two most commonly utilized techniques are intracavitary and interstitial. In intracavitary brachytherapy, the radionuclide is placed in a special applicator inside a body cavity. In interstitial HDR brachytherapy, the source is placed inside the tumour via surgically implanted catheters. [2]. The treatment modality enables enhanced localized dose delivery to the target, offering

improved conformal therapy with a sharp dose fall-off outside the target volume. This feature effectively minimizes the dose to the nearby organs at risk (OARs). However, due to the rapid dose fall-off, precise delivery protocols and efficient quality control programs become essential, as even slight source displacements can lead to large dosimetric variations. [3].

2.1.1 Dose Rate

One of the most common ways to classify brachytherapy is through the dose rate at the point prescribed [4]. There are three classifications for dose rates: low-dose rate (LDR), medium-dose rate (MDR) and high-dose rate (HDR). LDR procedures, which commonly use ¹²⁵I, ¹⁰³Pd and ¹³¹Cs as the radioactive sources, deliver dose at the rate of 0.4-2 Gy/h, requiring treatment times of 24-144 h [5]. MDR procedures are classified as delivering doses at the rate of 2–12 Gy/h and are not commonly used in the clinic. Lastly, HDR procedures deliver a dose at a rate greater than 12 Gy/h and can only be delivered using a remote afterloader for the safety of the patient and clinicians due to the sources used having high activities [5]. Treatment times are on the scale of minutes, which is its most important advantage. The full procedure is usually completed with 4-6 fractions [6]. It also has cost benefits compared to the other procedures, as multiple patients can be treated with a single source if the activity is acceptable.

2.1.2 Dosimetry

In conventional brachytherapy practice, the absorbed radiation dose is calculated and reported as dose to water in water (Dw,w) according to the recommendations provided by American Association for Physicists in Medicine (AAPM) Task Group No. 43 (TG-43) [7, 8]. Treatment planning systems (TPS) typically model the human body as a water sphere with unit density. The TG-43 dose calculation formalism describes the dose deposition around a single source placed centrally in a spherical water phantom. However, certain factors such as tissue and applicator heterogeneities, intersource attenuation (for LDR brachytherapy), and finite patient dimensions are not taken into account in this calculation method. Its line source geometry assumes evenly distributed radioactivity along a 1D line segment. It can also be simplified to a point source that assumes a spherical symmetry dose distribution at a given radial distance. It can be expressed by the following equation:

$$D(r,\theta) = S_K \cdot \Lambda \cdot \frac{G_X(r,\theta)}{G_X(r_0,\theta_0)} \cdot g_X(r) \cdot F(r,\theta)$$
(2.1)

Where r_0 and θ_0 correspond to the reference distance and polar angle relative to the source longitudinal axis, as illustrated in Figure 2.1, which is 1 cm away from the source center at 90°. r and θ correspond to the point of interest denoted as $P(r, \theta)$ in Figure 2.1. The subscript "X" indicates whether the model used is a point or line source.

The air-kerma strength, S_K , is the air-kerma rate, $\dot{K}_{\delta}(d)$, in vacuo (measurements corrected for photon interactions such as attenuation and scattering in the air between the source and detector and from any nearby objects) multiplied by the distance squared. The equation is,

$$S_K = \dot{K}_{\delta}(d) \cdot d^2 \tag{2.2}$$

The calculated air-kerma rate excludes low-energy that increase the value but do not contribute to the dose at distances greater than 0.1 cm in tissue. This energy cutoff for

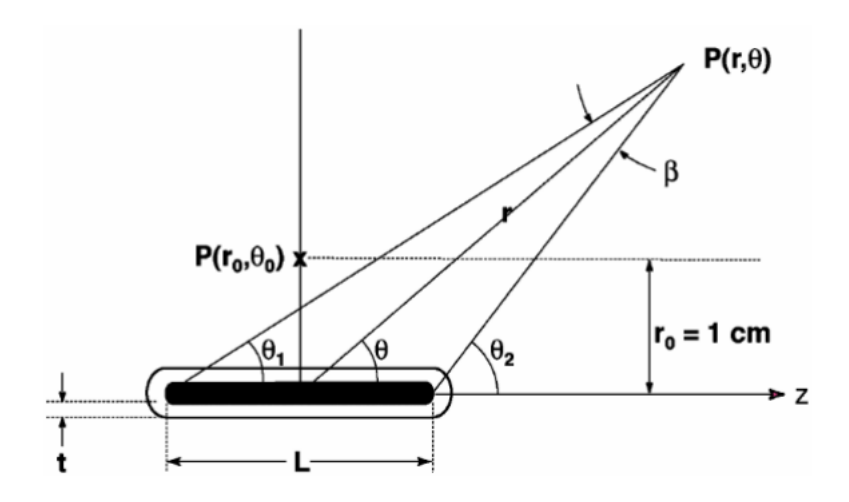


Figure 2.1: Brachytherapy dosimetry coordinate system

low-energy photon emitting sources used in brachytherapy is typically 5 keV [8].

The dose rate constant in water, Λ , is the ratio of the dose rate at the reference point in water to the air-kerma strength, which can be observed in the equation:

$$\Lambda = \frac{\dot{D}(r_0, \theta_0)}{S_K} \tag{2.3}$$

The value of this parameter is determined by both the element of the radioactive source and its dimensions, and it can also be influenced by the internal design of the capsule.

The geometry function, $G(r,\theta)$, neglects scattering and attenuation but is the correction for the inverse square law based on the assumptions made for the distribution of radioactivity for a point source or a line source. It is defined as,

$$G_P(r,\theta) = r^{-2} \tag{2.4}$$

$$G_L(r,\theta) = \begin{cases} \frac{\beta}{Lr\sin\theta}, & \text{if } \theta \neq 0^o \\ \frac{1}{r^2 - \frac{L^2}{4}}, & \text{if } \theta = 0^o \end{cases}$$
 (2.5)

where β is the angle enclosed by the tips of the line source seen in Figure 2.1 and L is the active length of the line source.

The radial dose function, $g_X(r)$ corrects for the photon scattering and attenuation contribution to the dose fall-off on the transverse plane. It is calculated using the equation,

$$g_X(r) = \frac{\dot{D}(r, \theta_0)}{D(\dot{r_0}, \theta_0)} \cdot \frac{G_X(r_0, \theta_0)}{G_X(r, \theta_0)}$$
(2.6)

The function is normalized at r=1 cm. As depicted in Figure 2.2, the behaviors of LDR sources and HDR sources display notable differences. The figure illustrates the significant dose gradient from the ^{125}I source (LDR source) primarily caused by dose deposition through the photoelectric effect alone. On the other hand, higher energy sources commonly used in HDR brachytherapy, such as ^{192}Ir , exhibit a rapid decrease in dose with distance from the source, which is offset by the contribution of scattered photons. This characteristic allows for a more uniform dose distribution for larger tumors compared to LDR treatments.

The 2D anisotropy function, $F(r,\theta)$, is greatly affected by the source dimensions as it describes the differences in dose as a function of polar angle relative to the transverse plane. It is calculated by,

$$F(r,\theta) = \frac{\dot{D}(r,\theta)}{D(\dot{r},\theta_0)} \cdot \frac{G_L(r,\theta_0)}{G_L(r,\theta)}$$
(2.7)

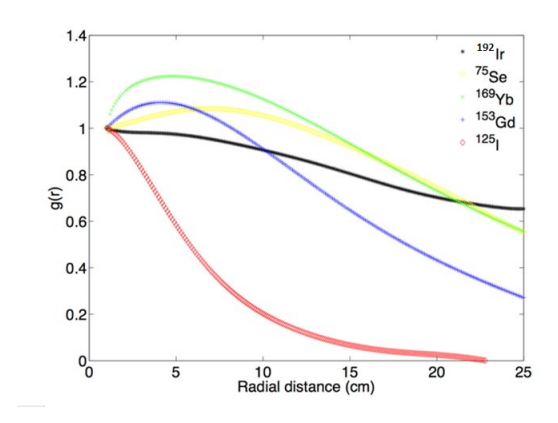


Figure 2.2: Radial Dose functions of five different radiation sources

The TG-43 formalism, while providing a standardized and fast method for dose calculation, is limited by its assumption of treating the patient as a homogeneous water medium [9]. This assumption can impact the accuracy of the final calculated results, particularly for sources with low and intermediate energies, where the photoelectric effect is prevalent. In these cases, the mass attenuation coefficients influence the dose distribution, which is not accounted for in the TG-43 formalism. Additionally, even for high energy sources, the scatter-to-primary ratio is at its maximum in low-Z materials [9]. As a result, the TG-43 formalism fails to consider tissue heterogeneity, leading to significant deviations between the expected and actual dose distributions in many cases. Anagnostopoulos et al. found that for esophageal HDR brachytherpy that there were no differences within the target volume, but revealed that the TG-43 calculated dose overestimated the dose to the spinal cord by 13% and underestimated the dose to the sternum bone by 15% [10]. Lymperopoulou et al. investigated HDR breast treatments and found that the TG-43 calculated dose was up to 10% larger compared to the prescribed dose for the lung, which was attributed to not only the lack of heterogeneity, but also to lack of good scattering

conditions [11]. To address these limitations, model-based dose calculation algorithms have been developed specifically for brachytherapy, and their application will be discussed in detail in the following section.

2.2 Model-based Dose Calculation

To achieve more accurate modelling of dose distributions in brachytherapy, model-based dose calculation algorithms (MBDCAs) are employed, which consider radiation interactions in non-water media. The three methods used presently to provide a detailed and accurate method for calculation of absorbed dose in heterogeneous systems such as the human body are the collapsed-cone superposition/convolution method, deterministic solutions to the linear Boltzmann transport equation and Monte Carlo simulations [9]. While these methods yield precise dose calculations when applied accurately, their practical implementation during treatments can be time-consuming, making them less suitable for real-time clinical use. Nonetheless, these methods are extensively utilized for research purposes. However, they encounter practical challenges, particularly their sensitivity to the dose specification medium and voxel-by-voxel Additionally, their practicality is further hampered by the interaction cross sections. uniqueness of each patient-source-applicator configuration, making it infeasible to have reference data for every potential combination. To address these issues, AAPM Task Group No. 186 report (TG-186) was published [9]. The report provides recommendations to enhance the use of MBDCAs in clinical practice.

One recommendation is that the TPS used with the MBDCA should have the capability to calculate the dose or dose rate in a homogeneous water phantom to allow

for a direct comparison with TG-43 parameters. To overcome the sensitivity to the dose specification medium, the report suggests avoiding the fixation of a reference medium such as water. Instead, it recommends reporting the dose to the tissue composing each voxel, allowing for a more comprehensive analysis. Lastly, with regards to voxel-by-voxel interaction cross sections, it recommends that organs be contoured and approved by radiation oncologists and that the tissue composition be assigned uniformly to this contour. TG-186 provides recommendations for assigning tissue elemental compositions for various organs and the nominal physical densities both acquired from ICRU No. 46 as a reference source [4].

In all MBDCA dose engines, there exists a trade-off between the uncertainty in dose calculations and the computational time required. Consequently, dealing with some degree of uncertainty is inevitable, and to reduce it, the computation time needs to be increased. TG-186 determined a threshold for acceptable uncertainty, and the time taken to achieve these results was carefully documented. Further discussion on these values will be presented in the thesis.

2.3 Intensity Modulated Brachytherapy

Brachytherapy is known for its superior conformal therapy compared to many other treatment modalities. The treatment can have shorter treatment times, decreased dose to healthy tissues and may be much more cost-effective than external beam radiotherapy with comparable outcomes [12, 13, 14]. However, it does have limitations as the sources used typically emit a rotationally symmetric dose distribution. This poses a challenge when optimizing treatment plans for irregularly shaped tumour lesions that require a high dose to the target area, often resulting in suboptimal target conformity [15]. To answer these

limitations in conventional brachytherapy, implementing highly attenuating materials in the applicators has been greatly investigated. This method is known as intensity-modulated brachytherapy (IMBT) and was originally investigated by Ebert *et al.* in 2002 [16].

The concept of dynamically rotating the highly attenuating material while irradiating the source allows the possibility to dynamically direct the radiation towards the tumours and away from the healthy tissue. The dose distributions will better conform to the tumour's shape, allowing the dose to escalate to the tumour while effectively shielding organs at risk (OAR). A systematic review was conducted by Callaghan *et al.* (2019) that analyzed all peer-reviewed journal articles on IMBT published between January 1, 1980 and January 1, 2019. The review identified 18 studies that successfully decreased the dose to OARs by 5.1-68.2%, demonstrating significant improvements in radiation protection for critical structures. 11 studies reported improved treatment planning and delivery times by 7.6-99.7%, highlighting the potential for enhanced efficiency and workflow optimization. Lastly, six studies increased target coverage by 18.6-71.6% relative to standard-of-care treatments, indicating improved tumour control [15].

Famulari et al. (2020) designed and manufactured an IMBT radiation delivery system prototype called AIM-Brachy to treat prostate cancer [17]. The AIM-Brachy system dynamically controls the rotation of MRI-compatible platinum shields placed within interstitial catheters, which partially collimate the radiation emitted from a ¹⁶⁹Yb source [18]. Platinum shields reduce the dose rate on the shielded side at 1 cm to 18.1% of the dose rate on the unshielded side. The AIM-Brachy system can create a low-dose tunnel within the urethra to minimize the occurrence and severity of urethral strictures or, alternatively, to provide a method for dose escalation as well as to decrease the side effects by minimizing the dose to the rectum and bladder. In a retrospective study, a dataset of 12

prostate cancer patients treated with external beam radiotherapy followed by HDR brachytherapy boost was used to generate conventional HDR brachytherapy and IMBT treatment plans using an in-house treatment planning system called RapidBrachyMCTPS [19, 20]. No margin was applied to the urethra contour. Given equal planning target coverage, IMBT has the potential to, on average, reduce the urethra D_{10} by $13.3\% \pm 4.7\%$ (range: 4.1-20.6%) without affecting other plan quality indices. D_{10} is the minimum dose received by the "hottest" 10% of the urethral volume and is associated with urinary toxicity.

Morcos and Enger (2020) developed an intracavitary IMBT delivery system for the cervix [21]. An MRI and CT compatible tandem (outer diameter 6 mm, inner diameter 3 mm) and ring applicator (Elekta Brachytherapy, Veenendaal, The Netherlands) was redesigned to enable a rotating shield. To maximize the amount of shielding material in the tandem, its inner diameter was changed to 5.4 mm. The 5.4 mm thick tandem shield resembles a flute due to the 1 mm diameter beam collimation holes spaced 10 mm apart along its outer surface, which in addition to collimating the beam laterally, limits dose to organs at risk above and below the dwell position. The shield is connected to the rotating IMBT delivery system through a custom miniature joint, which enables the transfer of rotational force while maintaining the bend required for the angled tandem. The lunar ovoids are unshielded and left unchanged. Tungsten was chosen as the shield material due to its relatively high density and exhibition of minimal magnetic susceptibility artifacts in MRI-based brachytherapy and clinically acceptable metal artifacts in CT imaging. To investigate the benefits of this system, data from 36 cervical cancer patients were considered in a retrospective IRB-approved study [22].

14 implants were performed with the Venezia hybrid applicator. The Vienna-style

hybrid tandem and ring applicator was used on the remaining 22 cases. All implants were performed under MRI guidance. Hybrid intracavitary/interstitial brachytherapy implants combined with 3 to 6 needles were used for six cases. All patients received external beam radiotherapy in 25 fractions at 1.8 Gy/fraction followed by 5 fractions of HDR brachytherapy boost using 5.5 Gy/fraction. The IMBT tandem was set to rotate at 22.5° increments. Each IMBT case was simulated using the three radionuclides ¹⁹²Ir, ⁷⁵Se and ¹⁶⁹Yb. ¹⁹²Ir and ⁷⁵Se-based IMBT represents a superior alternative to conventional intracavitary HDR brachytherapy with even greater improvements with ¹⁶⁹Yb. Compared to intracavitary/interstitial HDR brachytherapy, needle-free IMBT with ¹⁶⁹Yb improved tumour coverage and OAR sparing; ⁷⁵Se proved non-inferior; and ¹⁹²Ir led to clinically acceptable plans. Delivery of a conformal OAR-sparing dose without a single interstitial needle is an exciting avenue toward improving local control and reducing the morbidity of treatment for this group of patients.

IMBT holds great promise for improving treatment outcomes, minimizing radiationrelated side effects and enhancing overall patient care in brachytherapy. Continued research and technological advancements in IMBT have the potential to revolutionize the field further, leading to more personalized and effective treatment strategies.

2.3.1 High Dose Rate Endorectal Brachytherapy

At the Jewish General Hospital in Montreal, Canada, HDR endorectal brachytherapy is performed on patients with locally advanced rectal cancer. The procedure is CT-based image-guided and can be administered as a boost in three weekly fractions with a prescribed dose of 10 Gy to the clinical target volume (CTV) or as a standalone



Figure 2.3: Cross-sectional view of cylindrical intracavitary mold applicator (left) with the full assembly (right).

pre-operative treatment in four daily fractions with a prescribed dose of 6.5 Gy to the CTV [23, 24]. Presently, the cylindrical intracavitary mould applicator (ICMA) (Nucletron/Elekta; Veenendaal, the Netherlands) is used for this procedure, seen in Figure 2.3. The ICMA features an 8 mm diameter central channel designed to insert a highly attenuating material, surrounded by eight equally distributed catheter channels. Our lab is developing an applicator with a dynamically rotating shield to improve treatment outcomes.

As described above, significant dosimetric improvements are achievable with collimated brachytherapy sources, but practical challenges have impeded the clinical implementation of IMBT. For example, shields must be able to attenuate the intensity of the source significantly, preferably by several half-value layers, yet must be small enough to be used inside brachytherapy applicators and needles. However, a lower degree of attenuation that still improves achievable dose distributions can also be beneficial. This is possible for intracavitary HDR brachytherapy, but with respect to interstitial HDR brachytherapy, ¹⁹²Ir has too high of an energy to allow for adequate shielding within a small diameter of interstitial catheters. This necessitates alternative lower energy radiation

sources.

2.4 Desirable Characteristics of Brachytherapy Sources

Desirable characteristics for a radiation source used in brachytherapy include low mean gamma energy, long half-life, the feasibility of manufacturing into small capsules, and the ability to provide a suitable dose rate and distribution within acceptable treatment times. A low mean gamma energy is advantageous as it reduces the depth of penetration, resulting in a reduced dose to healthy tissue located farther from the source [25]. Additionally, lower gamma energies enhance the effectiveness of shields in protecting contra-lateral healthy tissues. Moreover, brachytherapy suites require less shielding, leading to reduced implementation costs for facilities [26]. A longer half-life for the radiation source is beneficial regarding cost and clinical workflow. It reduces the frequency of source replacement, resulting in cost savings and fewer source purchases. Fewer source The affordability of the source is an essential factor, calibrations are also required. influenced by the half-life and the method used to produce the radiation source, such as utilizing a nuclear reactor or a cyclotron. Sources manufactured using a cyclotron tend to be more expensive than those created using a nuclear reactor. Another disadvantage of using the cyclotron is that the radioisotopes produced are neutron deficient, causing them to have much shorter half-lives compared to ones produced in nuclear reactors [27]. The feasibility of manufacturing the source in small capsules is important for brachytherapy applications. The sources must fit into the small catheter channels present in applicators.

Despite their small size, they still need to deliver a sufficiently high dose to irradiate tumours in an acceptable treatment time effectively. The source's specific activity is the characteristic that allows for small source sizes.

Currently, the most commonly used HDR source in brachytherapy is 192 Ir, ($E_{\gamma,av} = 360 \text{ keV}$, half-life = 74 days). The manufacturing of 192 Ir sources for brachytherapy has been optimized, utilizing well-known assembling and welding techniques [28]. This optimization enables the production of high-specific activities, resulting in dose rates that allow for short treatment times (typically less than 15 minutes). The half-life is tolerable for most clinics, and while its gamma energy is not extremely low, it is lower compared to alternative sources presently used. For clinics that may not be able to accommodate the short half-life of 192 Ir due to cost and/or transportation time, 60 Co ($E_{\gamma,av} = 1250 \text{ keV}$, half-life = 5.3 years) is often used. 60 Co has a significantly higher average gamma energy. However, with such a long half-life, the source rarely needs to be replaced, allowing for a great reduction in cost.

For HDR brachytherapy to be effective, low energy radioisotopes ($E_{\gamma,av} < 50 \text{ keV}$) [9] are not considered as they have short half-lives and are not capable of producing dose rates that are comparable to ¹⁹²Ir. Intermediate-energy radioisotopes (50 keV > $E_{\gamma,av} < 200 \text{ keV}$) [9] have been investigated for use in brachytherapy applications, which include ¹⁷⁰Tm [29, 30], ¹⁵³Gd [31], ¹⁶⁹Yb [32, 33, 17] and ⁵⁷Co [34]. It was found that each one has some disadvantages that cause the source to be impractical for clinical applications. For ¹⁷⁰Tm, at depths less than 5 mm, it has considerable bremsstrahlung and beta contamination [29]. The source's practically achievable dose rate is also significantly lower than that of ¹⁹²Ir [35], meaning that either the source dimensions need to be significantly larger or the irradiation time needs to be longer to achieve an equivalent dose rate to ¹⁹²Ir. The dosimetric characteristics of ¹⁵³Gd allowed a theoretical source to be designed. However, the manufacturing process

was unfeasible, rendering the source incapable of clinical use [36]. ¹⁶⁹Yb has a short half-life of 32 days, which is too short when considering the production and delivery time. Lastly, the production of ⁵⁷Co is prohibitively expensive, as the technique to achieve an equivalent dose rate to ¹⁹²Ir requires a 1-2 mA cyclotron to function for many thousands of hours [37].

This research led to the decision to look into high-energy radioisotopes that had mean gamma energies less than 192 Ir (200 keV > $E_{\gamma,av}$ < 360 keV) [9]. 75 Se ($E_{\gamma,av}$ = 215 keV, half-life = 119 days) exhibited the desirable characteristics of a brachytherapy source with a lower mean gamma energy and a longer half-life, so it was selected for further investigation.

2.4.1 Selenium-75

⁷⁵Se is a commonly used radioisotope in industrial radiography for inspecting infrastructure defects, including steel beams and oil pipelines. Its performance advantages compared to ¹⁹²Ir makes it a preferred choice for applications that have metal thicknesses of 5-30 mm [38]. Despite its favourable dosimetric properties, the manufacturing aspects of elemental selenium can pose challenges. Elemental selenium is highly toxic, volatile, reactive and corrosive. It also has a very large coefficient of expansion close it its melting point of 217 °C, and to avoid contamination during production, it requires encapsulation of the element prior to irradiation [39]. To address these manufacturing difficulties, various irradiation techniques, including different encapsulation methods and selenium compounds, have been investigated [40, 41, 39]. Although these techniques have been applied in industrial radiography source manufacturing, they have not been extensively applied to the production of brachytherapy sources. This limitation is primarily attributed to the size restrictions imposed by clinical applications, as brachytherapy sources have approximately

four times smaller diameters, and the safety concerns associated with placing the source inside a patient. Consequently, most existing literature analyzing the use of selenium in a brachytherapy setting is largely theoretical [26, 24, 42]. These circumstances have motivated us to delve deeper into these manufacturing solutions, leveraging our expertise to design, test, and manufacture a ⁷⁵Se brachytherapy source for clinical implementation.

2.5 Radiochromic Film

The specific radiochromic film used in this thesis was external beam therapy (EBT) GAFCHROMICTM film. The purpose of the film's use was to measure the physical dose emitted by the source manufactured and compare the results to doses acquired through simulations using an MBDCA. The film design consists of a 175 μ m polyester coated with a 28 μ m active layer film over which a 5 μ m topcoat is applied [43]. The film contains a special dye that is polymerized and develops a blue colour upon exposure to radiation. This causes there to be a change in optical density proportional to the amount of energy deposited that can be measured in a flatbed document scanner [44]. EBT GAFCHROMICTM film has been used in multiple brachytherapy applications [45, 46, 47]. It has the advantages of having a high 2D spatial resolution, being safe to handle in room light, being nearly tissue equivalent, having no angular dependence, being water resistant, allowing for use in water phantoms and that they can be custom cut depending on the application. Accurate film dosimetry requires controlling many variables such as scanning in the same lateral and longitudinal orientation for all scans, including the calibration scans that are used to relate optical densities to known doses.

Chapter 3

Manufacturing of a Selenium-75 brachytherapy source

Jake Reid $^{1,4},$ Jonathan Kalinowski $^{1,4},$ Hamed Bekerat 1, John Munro III 2, Andrea Armstrong 3, Shirin A. Enger 1,4

¹Medical Physics Unit, Department of Oncology, Faculty of Medicine, McGill University, Montreal, Québec, Canada

²Burnley Technology Inc., 380 Lafayette Road, Unit 11-162, Seabrook, New Hampshire 03874, USA

³McMaster University, Nuclear Operations and Facilities, Hamilton, Ontario, Canada

⁴Lady Davis Institute for Medical Research, Jewish General Hospital, Montreal, Quebec, H3T 1E2, Canada

3.1 Abstract

Background: 75 Se ($t_{1/2} = 119$ days, $E_{\gamma,avg} = 215$ keV) offers advantages over 192 Ir ($t_{1/2} = 74$ days, $E_{\gamma,avg} = 360$ keV) as a brachytherapy source due to its lower gamma energy and longer half-life. However, despite its widespread use in industrial gamma radiography, commercial fabrication of 75 Se brachytherapy sources is currently limited by manufacturing constraints. **Purpose:** This feasibility study aimed to manufacture and irradiate a low activity 75 Se brachytherapy source and perform measurements to assess its potential for brachytherapy applications.

Methods: A source was designed, and its TG-43U1 formalism was employed using the Monte Carlo-based treatment planning system, RapidBrachyMCTPS. A vanadium diselenide compound was encapsulated within a titanium capsule to create an active core with specific dimensions. The 75 Se source was irradiated at the McMaster Nuclear Reactor for 23.97 hours at an average neutron flux of 7.77×10^{13} n/cm²s to achieve an activity of 50 mCi. Source activity was measured using the AtomLab 500 detector. Gamma spectroscopy data were collected and analyzed using a high-efficiency HPGe ORTEC detector fitted with a lead shield to evaluate contaminants produced by vanadium and titanium.

Film measurements were conducted and compared with Monte Carlo simulations, with multiple films placed at different distances from the source within a solid water phantom. A gamma pass rate of 2%/2 mm was used to compare dose distributions between film measurements and Monte Carlo simulations. Correction factors were applied to compensate for uncertainties in the measurement setup.

Results: The air kerma strength per unit activity and dose rate constant were determined as $4.751 \pm 0.005 \times 10^{-8}$ U/Bq and 1.116 ± 0.001 cm⁻², respectively. These values

indicated that 75 Se would require an activity of 2.05 ± 0.1 times greater than a 10 Ci 192 Ir source to achieve a similar dose rate to water at 1 cm from the source along the transverse axis. The measured activity of the source was 20.3 mCi, which was lower than the expected value by over 50%. The radioactive contaminants from vanadium and titanium did not exceed 1% of the dosimetric contributions of 75 Se. Applying appropriate correction factors, a gamma pass rate of 95% was achieved for all films.

Conclusions: A low activity ⁷⁵Se brachytherapy source was successfully manufactured and irradiated. The calculated brachytherapy dosimetry parameters using the TG-43 formalism demonstrated the potential of the source as an alternative to ¹⁹²Ir. Post-irradiation measurements confirmed the integrity of the source and provided further evidence of its viability for brachytherapy applications. These findings support the need for further investigation into manufacturing methods and pave the way for future steps in bringing the source to clinical use.

3.2 Introduction

3.2.1 Brachytherapy

In high dose rate (HDR) brachytherapy, a sealed highly radioactive photon-emitting source (a seed), is temporarily placed inside or near the tumour. Owing to the steep dose gradients from brachytherapy sources, a high dose can be delivered to the tumour while minimizing the dose to the surrounding healthy tissues. Due to this distinctive characteristic, HDR brachytherapy is one of the most effective and precise radiation delivery modalities for certain tumour types, especially with image guidance [14, 48, 49, 50, 51, 52].

The major drawback of brachytherapy lies in its rotationally symmetric dose distribution from brachytherapy sources. While it effectively delivers a high dose to the tumour, it often lacks tumour conformity due to the non-symmetrical shape of tumours, resulting in radiation spillage to nearby healthy tissues. Several groups have addressed this issue by introducing metallic shields capable of rotating inside brachytherapy catheters and applicators. This innovative approach, called intensity-modulated brachytherapy, allows targeted radiation delivery towards the tumour while shielding surrounding healthy tissues. By dynamically directing radiation toward the tumour and away from healthy tissues, more effective tissue shielding can be achieved, and if necessary, allowing dose escalation inside the tumour. [17, 22, 21, 53, 54, 15]. Through theoretical calculations, these novel methods have shown better target coverage (18.6 %-71.6%) and decreased normal tissue dose (5.1%-68.2%) [55, 56, 57, 58, 59, 60, 61]. However, the practical implementation of IMBT faces challenges. The shields used in IMBT must efficiently attenuate the source's intensity, ideally by several half-value layers, while also being small enough to fit inside brachytherapy applicators and catheters. However, even a lower degree of attenuation, improving dose distributions, can be beneficial. In HDR brachytherapy, the current sources used are ¹⁹²Ir $(E_{\gamma,av} = 360 \text{ keV}, \text{ half-life} = 74 \text{ days})$ and ⁶⁰Co $(E_{\gamma,av} = 1250 \text{ keV}, \text{ half-life} =$ These sources are chosen for their high dose rates, cost-effectiveness, and practicality in manufacturing. However, their gamma energies are too high for the shields to effectively attenuate their dose by several half-value layers. Therefore, several alternative investigated brachytherapy lower-energy sources have been for applications [31, 36, 17, 34, 62, 18, 29, 30, 32, 33].

3.2.2 Selenium-75

For a novel radiation source to be considered a viable alternative to the currently used brachytherapy sources, it should possess certain characteristics. These include generating lower gamma energy photons, having a longer half-life, producing similar dose rates to allow for comparable treatment times, being feasible and cost-efficient to manufacture. Thus far, multiple intermediate energy isotopes (50 keV > $E_{\gamma,av}$ < 200 keV) have been investigated for use in brachytherapy applications [31, 36, 17, 34, 62, 18, 29, 30, 32, 33]. Clinical implementation of these sources was deemed unfeasible due to limitations such as high production costs, low specific activities and short half-lives. ⁷⁵Se ($E_{\gamma,av} = 216$ keV, half-life = 119 days) is a source that fits the criteria above.

⁷⁵Se is a radioisotope widely used for industrial gamma radiography. Its relatively low gamma energies and long half-life provides better images, fewer source exchanges and a cost reduction compared to presently used isotopes in this field, such as ¹⁹²Ir [38]. These same characteristics make it of interest for use in HDR brachytherapy. Several studies have theoretically analyzed ⁷⁵Se as a potential source for brachytherapy applications assuming pure elemental selenium is encapsulated. The studies demonstrated the benefits of the lower gamma energy with regards to the applicator shielding as well as a reduction in necessary room shielding in brachytherapy suites [26, 42, 24]. Most studies conducted on ⁷⁵Se have investigated the manufacturing and dosimetric properties of the source for use in industrial gamma radiography [40, 41, 38, 39]. These studies discuss the benefits of the source when in use, especially for acquiring better images of infrastructure [38]. However, they also discuss the difficulty in manufacturing ⁷⁵Se.

The two main difficulties in manufacturing ⁷⁵Se is (1) elemental selenium is highly toxic, volatile, reactive, corrosive with a very large coefficient of expansion close to its low melting point of 217 °C [39] and (2) the elemental selenium powder needs to be encapsulated prior to irradiation in comparison to other radioisotopes that can be encapsulated post-irradiation [40, 41]. If handled improperly, it can lead to explosions, fires and the production of harmful gases [63]. To address the first constraint, for industrial radiography, which does not require the source encapsulation to be as compact as for brachytherapy applications, many designs have been fabricated [40, 41, 38]. For these designs, the methods included encapsulating the elemental selenium twice, once prior to irradiation and the other post-irradiation. Another method to address this concern was introduced by Shilton (2000) using a selenium compound with an element more stable than selenium [39]. The main compound is vanadium diselenide, which makes the source less of a safety concern when irradiating.

In the case of ¹⁹²Ir, the production process involves its activation in a reactor, followed by encapsulation in stainless steel. Stainless steel is selected as the encapsulation material due to its malleability and cost-effectiveness, making it an ideal choice for encapsulating radioisotopes. However, in the case of selenium, it is essential to encapsulate it before irradiation, as mentioned earlier [40]. The irradiation process of the capsule in the nuclear reactor poses significant limitations on the choice of materials used. Many materials can chemically react with selenium and cause deformations in the capsule. Additionally, the production of radioactive contaminants may occur in the capsule, leading to the source being considered unsealed and affecting the dose distribution of the source. The joint American Association of Physcists in Medicine (AAPM) and European Society for Therapeutic Radiology and Oncology (ESTRO) task group 167 report recommends that radiation contaminants should be less than 5% of the dosimetric contributions of the

primary radionuclide [64]. Stainless steel contains iron, chromium and nickel, which will produce radioactive contaminants and is not stable enough to avoid deformation in the reactor. Therefore, selecting an encapsulation material that remains unactivated with the thermal neutron fluxes to which the source is exposed during irradiation is important.

3.2.3 Objectives

The aim of this study was to manufacture a ⁷⁵Se brachytherapy source and investigate its potential for use in brachytherapy applications. To accomplish this, a theoretical ⁷⁵Se brachytherapy source was designed and analyzed by (1) characterizing the source with the clinically relevant TG-43 formalism [7, 8], (2) manufacturing and irradiating the source and taking spectroscopy data to analyze radioactive contaminants and (3) performing proof of principle measurements with measurement-to-calculation agreement of a dose difference/distance to agreement criterion of 2%/2 mm by delivering ⁷⁵Se dose distributions to solid water phantoms.

3.3 Materials and Methods

In this study, a brachytherapy source containing ⁷⁵Se was designed and characterized using RapidBrachyMCTPS, a validated research treatment planning system available to the brachytherapy community upon request. RapidBrachyMCTPS offers a user-friendly graphical interface along with dose optimization, contouring, and dose analysis tools. It also incorporates an advanced Monte Carlo dose calculation engine known as RapidBrachyMC, and recently, a TG-43 parameter calculation module called RapidBrachyTG43 [19, 20, 65]. Following the design phase, the source was manufactured

and subsequently irradiated at the McMaster Nuclear Reactor, where its quality assurance and measurements were conducted. Calculations were performed using RapidBrachyMCTPS to validate the results, and a comparison was made with the measured values using the gamma index with a 2 mm distance-to-agreement and a 2% dose difference criterion. Detailed information on these steps is provided in the following sections.

3.3.1 Source Design and Characterization

The source design and encapsulation dimensions are illustrated in Figure 3.1. To achieve a volume of 2 mm³ as recommended by Weeks and Shulz for a 23 Ci ⁷⁵Se source [26], the length of the ⁷⁵Se source was increased compared to the currently utilized brachytherapy sources in clinical practice. While an activity of 23 Ci was chosen, to match the dose rate of a 10 Ci ¹⁹²Ir source, a 20.5 Ci ⁷⁵Se source would be needed. For dimensions of the source, all were kept similar to currently used brachytherapy sources except the length was extended to 7 mm while ensuring compatibility with existing applicators and 6F catheters commonly employed in brachytherapy applications with ¹⁹²Ir. Although longer sources may raise safety concerns due to the potential risk of getting stuck in catheters during treatments, a 7 mm source used in intracavitary brachytherapy is unlikely to get stuck. However, rigorous testing will be necessary to avoid any future complications.

This study uses the RapidBrachyTG43 module of the RapidBrachyMCTPS to characterize the source and calculate the radial dose function, 2D anisotropy function, air kerma strength per unit activity, and dose rate constant of ⁷⁵Se. The dose rate per activity to water at 1 cm from the source along the transverse axis was calculated using the TG-43

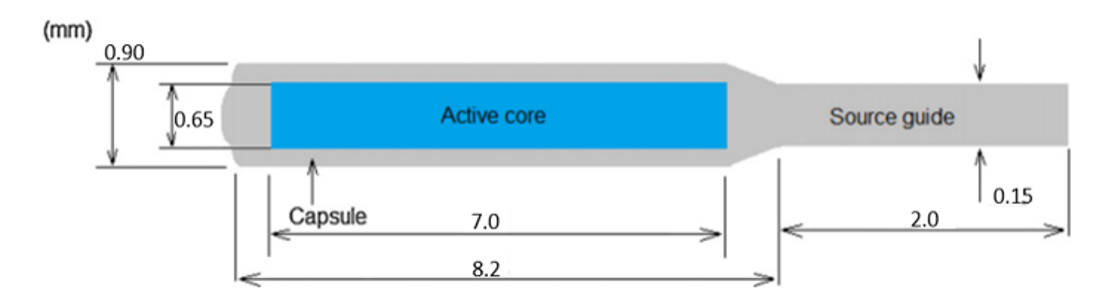


Figure 3.1: Geometric design of the ⁷⁵Se theoretical source with dimensions given in millimeter.

formalism, simply as the product $\frac{S_K}{A} \times \Lambda$ for both $^{75}\mathrm{Se}$ and $^{192}\mathrm{Ir}.$

3.3.2 Source Manufacturing

An inert source was manufactured in collaboration with Spectrum Safety Inc. (Lowell, Massachusetts). A ⁷⁴Se source target was developed by first compounding ⁷⁴Se enriched to greater than 99.5% with naturally occurring vanadium. An overall description can be found in the patent completed by Shilton [39]. The compound VSe₂ was ground into a fine powder and pressed in a 0.6 mm die at approximately 965 MPa. The resulting pellets had an average length of 2.5 mm and a density of 4.95 mg/mm³. A 10 mm long pure titanium tube with dimensions of an outside diameter of 0.965 mm and an inside diameter of 0.686 mm was laser welded closed on one end. Then three pellets totalling 7 mm in length were inserted into the tube. A piece of commercially pure titanium wire 0.5 mm diameter was inserted into the tube and laser welded in place, sealing the tube. The wire was then trimmed so that 10 mm protruded from one end of the source target. This titanium protrusion was used for source handling.

The inert source was then irradiated at McMaster Nuclear Reactor. An irradiation

capsule containing the brachytherapy source, a vanadium piece (0.2154 g), a titanium wire piece (0.0168 g) and a Co-Al wire piece (1% Co, 0.0113 g) were capped in a quartz tube separately wrapped in aluminum foil, which was placed in-core. The capsule was placed in a part of the reactor that experiences a thermal neutron flux to activate ⁷⁴Se more than vanadium and titanium, as these elements activate in fast neutron fluxes. The Co-Al wire piece determined the average neutron flux during irradiation. The vanadium and titanium wire pieces were placed in the capsule to investigate the radiation contaminants. The capsule was irradiated for 23.97 h to achieve an expected activity for the source of 50 mCi. This activity was chosen to allow source positioning to be completed manually, as the source could not be placed in a remote afterloader. The activity measurements of the brachytherapy source and Co-Al wire were completed using the AtomLab 500 detector.

To analyze the contaminants produced by vanadium and titanium, the collection and interpretation of gamma spectroscopy data were completed. The two samples were characterized by gamma spectroscopy using a high-efficiency HPGe ORTEC detector fitted with a lead shield to eliminate background noise. A spectrum was recorded two days after the end of bombardment and again four days later, to verify peak assignments based on changes in intensity. Radionuclides were identified by gamma energies, presence of correlated lines in expected relative intensities and half-life measurements. Once identified, the radionuclides were quantified by correcting each gamma line's relative intensity from the Live Chart of Nuclides [66] and detector efficiency at that energy. This provided the activity of each radionuclide present at the time of the count, which was then decay corrected to the end of irradiation. The data was then analyzed to produce tables showing the radionuclide impurities per milligram of material for each metal at the end of the bombardment.

The efficiency curve used for correction was constructed for the HPGe ORTEC

detector using a NIST multi-gamma disc source. This was created by taking the current activity of the disc source from its reference date and value using the standard radioactive decay equation. The apparent counts per second at the energies listed on the certificate were recorded. Each apparent count per second was divided by the actual disintegrations per second to determine the efficiency of that energy.

3.3.3 Film Measurements

Physical Setup

Film measurements were obtained using EBT3 Gafchromic film, placed in a solid water phantom comprising 14 slabs (Figure 3.2). All slabs were 30 x 30 cm² and varied in thickness to create different distances between the source and the film. A contraption was used to hold all slabs together to ensure parallel alignment and matching corners. The central slab, 1 cm thick, had catheter holes drilled into it, with the center hole holding the source. Additionally, two outer slabs, 6 cm thick, were positioned to mimic backscattering conditions.

Various slabs with different thicknesses were placed strategically to achieve specific source-to-film distances of 0.5, 0.7, 1, -1, -1.2, 1.5, -1.6, 2, and -2.6 cm. These distances were selected to enable a comprehensive analysis of the source's dose distribution. The chosen range of distances allowed the film to analyze doses between 0.25 to 40 Gy effectively.

Prior to source irradiation, the measurement setup was CT scanned to verify that the source was centred and to have the necessary data to complete Monte Carlo simulations using RapidBrachyMCTPS properly. After irradiation, the film was taped onto each slab at the proper distances. The activity of the source was then read from the



Figure 3.2: Measurement setup for film measurements. Solid water phantom is located behind lead bricks for radiation safety. The films were placed and centered on each slab.

AtomLab 500 detector, and an irradiation time of 20 hours was decided. The source was wrapped in a plastic wrap to avoid potential contamination between the source and the solid water phantom slabs. The films were then brought to two separate scanners at the Jewish General Hospital, EPSON 10000XL and EPSON 11000XL (Seiko Epson Corporation, Nagano, Japan), which provide 48-bit RGB images. Two separate scans were completed for ten films, including a film that received no dose to analyze background radiation. Before these scans, both scanners had multiple films scanned with known doses created from an orthovoltage beam to compute a calibration curve for film analysis. The calibration curve was created using the methods stated in the study conducted by Lewis et

al. [67]. The calibration and measurement films were scanned within 24 hours after irradiation with 50 dpi corresponding to 2.0 mm/pixel. All films were labelled and scanned in landscape orientation as the rotation of the scanner bed can lead to significant differences in measured signal [68].

Monte Carlo Simulations

To validate the accuracy of the dose distribution obtained from the film measurements, we utilized the software RapidBrachyMCTPS to simulate the irradiation of the ⁷⁵Se source within the same solid water phantom used in the film measurements. The simulation results were then compared with the measured data from the film for validation. Specifically, for this simulation, DICOM images of the measurement setup, acquired from the CTcompleted prior irradiation, scan to source were imported intoRapidBrachyMCTPS. The drilled holes for source channels as well as the solid water phantom slabs were the only contours in the simulation. The material assignment of air was used for the source channel contours and PMMA was used for the solid water phantom contour. A single dwell position was placed in the source location in the central catheter channel. The dwell time was set to 20 hours. A $1 \times 1 \times 1 \text{ mm}^3$ scoring grid was chosen with 10^9 decays. These parameters allowed for there to be a Type A uncertainty of <0.5%within the 1 Gy 100% isodose line.

Voxellized representations of the measurement setup were inputted to RapidBrachyMC in egsphant format [69]. Material properties and densities were assigned via nominal material/density assignment to contours made for each component of the phantom (Appendix A). RapidBrachyMC utilizes the Geant4 Monte Carlo radiation transport toolkit [70, 71, 72], employing photon decay spectra from the Evaluated Nuclear

Structure Data File for simulation of radioactive decay [73]. The simulation was executed on the Cedar cluster of the Digital Research Alliance of Canada. Due to the low photon energies emitted by ⁷⁵Se, it was assumed that the secondary electrons deposit their energy locally [69], allowing the dose to be estimated through collision kerma, scored using a track length estimator [74]. Implementation of multi-threading in RapidBrachyMCTPS in conjunction with this method reduces the computation time. The Monte Carlo simulation parameters, seen in Appendix B, were summarized in accordance with the recommendations of TG-268 [75]. The history-by-history method was used to calculate the type A uncertainty on the absorbed dose per voxel [76].

A gamma index with a distance of agreement of 2 mm and a percent dose difference of 2% was used to compare the dose distributions between the physical measurements and the simulations. For there to be an agreement between dose distributions, the gamma index pass rate must be greater than 95%. Due to positional uncertainty from the measurement setup with regards to the air gaps between slabs and the source in the catheter channel as well as uncertainty in the source's activity with the use of the AtomLab 500 detector, correction factors were calculated that were within justification and were applied to the Monte Carlo dose distributions.

A film measurement taken at 1 cm was used to determine the source activity correction factor. Various source activity and film position combinations were iterated to identify the combination that yielded the highest gamma pass rate. The activity was iterated through a range of 1 to 1.5 times the originally measured activity value, considering that the measured value was likely underestimated. The position values were iterated through a range of 1 to 1.3 cm, considering that positional uncertainties would contribute by increasing the distance between the source and film. Once the activity

correction factor was calculated, it was applied to all film measurements, incorporating iterations for the position value ranging from the distance to 0.5 cm greater than the distance.

3.4 Results

3.4.1 TG-43U1 Parameters

Using RapidBrachyTG43 [65], the AAPM TG-43U1 brachytherapy dosimetry parameters for the 75 Se source were calculated. The radial dose function and 2D anisotropy functions were determined. The data can be seen in Figure 3.3. The air kerma strength per unit activity and dose rate constant for 75 Se were $4.751 \pm 0.005 \times 10^{-8} \text{ U/Bq}$ and $1.116 \pm 0.001 \text{ cm}^{-2}$, respectively. Using TG-43 formalism, these values were multiplied together to calculate the dose rate per activity to water at 1 cm from the source along the transverse axis. This value was determined to be 2.05 ± 0.1 times less than what 192 Ir produces.

3.4.2 Source Characteristics

Following a 23.97 hour irradiation period in the nuclear reactor, the measured activities of the 75 Se source and the Co-Al wire using the AtomLab 500 detector were 20.3 mCi and 34.2 μ Ci, respectively. The observed activity was more than 50% lower than the expected value, and the activity from the Co-Al wire indicated an average neutron flux of 7.77×10^{13} n/cm²s during irradiation.

The results of the contaminants analysis for the titanium and vanadium samples, after correction from the efficiency curve, are presented in Table 3.1 for the titanium sample

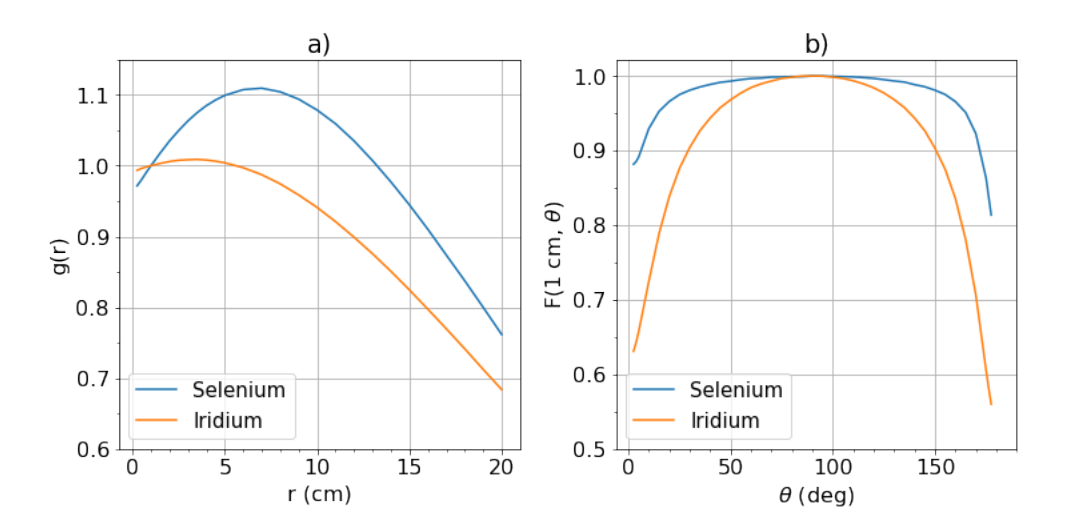


Figure 3.3: TG-43 parameter comparison between ⁷⁵Se and ¹⁹²Ir sources for a) the radial dose function and b) the 2D anisotropy function.

and Table 3.2 for the vanadium sample. The tables provide the measured activity for the respective masses used: 0.0168 g for titanium and 0.2154 g for vanadium. Additionally, extrapolation data is provided, indicating the activity per milligram of each element.

The exact masses of titanium and vanadium were unknown due to proprietary reasons, however, the total mass of the brachytherapy source was measured to be 37.6 mg, which includes a 10 mm titanium wire attachment for handling, and the mass of the ⁷⁵Se used was measured to be 7.41 mg. Using these values, the combined mass of vanadium and titanium is known to be 30.19 mg, allowing for calculations of the total contamination contribution for different mass combinations of the two elements. Through evaluation of various mass arrangements of titanium and vanadium, within the specified combined mass value, the radioactive contaminants never exceeded 1% of the dosimetric contributions of ⁷⁵Se.

Table 3.1: Radioactive impurities in titanium wire piece that weighed 0.0168 g. The table also contains extrapolation information for impurities per mg of sample. Very short-lived radionuclides will not appear in this spectrum due to the delay between end of bombardment and gamma spectrum acquisition.

Radionuclide	Activity (Bq)	Activity per mg of Ti (Bq/mg)
Na-24	6.25×10^{7}	3.72×10^9
Sc-46	2.21×10^4	1.31×10^{6}
Sc-47	8.79×10^{5}	5.23×10^{7}
Sc-48	2.06×10^{5}	1.23×10^{7}
Cu-64	1.26×10^{5}	7.49×10^{6}
Ga-72	6.30×10^{3}	3.75×10^{5}
As-76	3.45×10^4	2.05×10^{6}
Sb-122	2.31×10^4	1.37×10^{6}
Sb-124	5.34×10^{2}	3.18×10^4
La-140	1.74×10^{5}	1.04×10^{7}
Ho-166	1.25×10^{6}	7.47×10^{7}
Yb-175	1.41×10^4	8.37×10^{5}
W-187	7.56×10^{3}	4.50×10^{5}

Table 3.2: Radioactive impurities in Vanadium pieces that weighed 0.2154 g. The table also contains extrapolation information for impurities per mg of sample. Very short-lived radionuclides will not appear in this spectrum due to the delay between EoB and gamma spectrum acquisition.

Radionuclide	Activity (Bq)	Activity per mg of Ti (Bq/mg)
Na-24	2.18×10^{4}	1.01×10^{5}
K-42	9.73×10^{5}	4.52×10^{6}
Sc-47	3.81×10^{3}	1.77×10^4
Sc-48	2.74×10^{5}	1.27×10^{6}
Cr-51	3.30×10^4	1.53×10^{5}
Cu-64	2.97×10^{6}	1.38×10^{7}
Fe-59	3.99×10^{2}	1.85×10^{3}
Ga-72	2.81×10^{5}	1.30×10^{6}
Se-75	3.82×10^{4}	1.78×10^{5}
Br-82	6.84×10^{3}	3.17×10^4
Sb-124	1.12×10^{3}	5.21×10^{3}
Ho-166	4.34×10^4	2.01×10^{5}
W-187	4.07×10^{3}	1.89×10^4

3.4.3 Film

Figure 3.4 provides an example of the dosimetric comparison plots completed for all nine film measurement distances. The simulations have a Type A uncertainty of <0.5% for voxels within the 100% isodose line of 1 Gy.

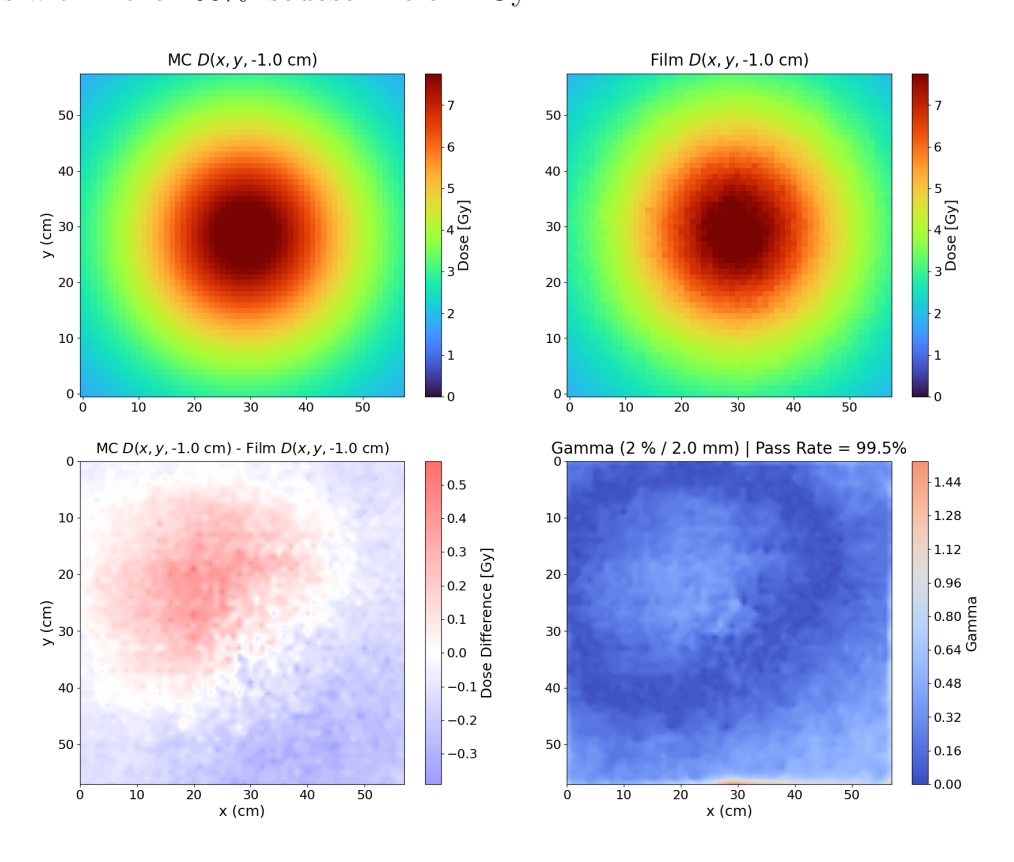


Figure 3.4: Dosimetric comparison plots for the -1 cm source to film distance between the Monte Carlo (top left) and physical film (top right) dose distributions. The absolute dose difference (bottom left) and gamma values (bottom right) are shown. The dwell time was set to 72000 s

Table 3.3 displays the final results for the film measurements using a source activity correction factor of 1.237. All gamma pass rates were above 95% with distance correction values that increased when the source-to-film distance increased.

Optimized Gamma Source to Distance Correction Pass at Film Distance Value (cm) Distance Value (cm) Max (%) (cm)0.5 0.1750.675100 0.7 0.28 0.98 100 1.325 1 0.32597.6 1.5 0.3251.825 99.5 2 0.3552.355 98.8 -1 -0.075-1.07599.5-1.2 -0.13-1.33 100 -1.6 -0.195-1.79596.7 -2.6-0.18-2.7899.8

Table 3.3: Film results achieved using a source activity correction factor of 1.237.

3.5 Discussion

The lower gamma energy and longer half-life of ⁷⁵Se, compared to the commonly utilized brachytherapy source, ¹⁹²Ir, make it a promising alternative for brachytherapy applications. It is hypothesized that the lower gamma energy of ⁷⁵Se holds the potential to minimize the dose absorbed by healthy tissues during brachytherapy treatments, thereby improving treatment plans and potentially enhancing the overall quality of life for patients. Furthermore, it is anticipated that using ⁷⁵Se may reduce the room shielding required in brachytherapy suites, reducing implementation costs. This notion supports the findings of a study conducted by Weeks and Schulz [26].

Despite the numerous advantages offered by ⁷⁵Se, its clinical utilization is presently constrained due to challenges associated with manufacturing small brachytherapy capsules that can deliver dose rates equivalent to those achieved with ¹⁹²Ir. In its elemental form, ⁷⁵Se exhibits high volatility and a significant expansion coefficient near its melting point of 217

°C. Moreover, ⁷⁵Se necessitates encapsulation before irradiation in a nuclear reactor, risking activation of the capsule material, which introduces additional complexities compared to the post-irradiation encapsulation of ¹⁹²Ir. To address these safety concerns, a vanadium diselenide compound was formulated based on the guidance of the patent developed by Shilton [39], and titanium was chosen as the capsule material. The vanadium diselenide compound was chosen as the addition of vanadium to the source brings stability during the manufacturing and irradiation process, while minimally impacting the dose distribution of the source. Titanium was chosen as the capsule material due to it having a natural form being composed of five stable isotopes: 8% ⁴⁶Ti, 7.3% ⁴⁷Ti, 73.8% ⁴⁸Ti, 5.5% ⁴⁹Ti and 5.4% ⁵⁰Ti [77]. This material is expected to produce radioactive contaminants (i.e. scandium isotopes), however it is activated in fast neutron fluxes, whereas selenium is activated in thermal neutron fluxes.

In this study, a ⁷⁵Se source with dimensions similar to currently used brachytherapy sources was designed. Its TG-43 parameters were calculated. The source was manufactured and irradiated at the McMaster Nuclear Reactor. The post-irradiation results provided a proof of concept of a ⁷⁵Se brachytherapy source, as the source remained intact without deformations and exhibited acceptable radiation contaminants for brachytherapy treatments from the vanadium and titanium elements. Although the activity of the source, as measured by the AtomLab 500 detector, was lower than the expected value, film measurements could still be completed within a reasonable time frame. The dose distributions obtained from physical film measurements and Monte Carlo simulations exhibited good agreement.

3.5.1 TG-43 Calculations

In this paper, the TG-43 parameters of ⁷⁵Se were calculated and compared to ¹⁹²Ir. In Figure 3.3a, it can be seen that ⁷⁵Se has a similar radial dose function as ¹⁹²Ir. The functions increase above a value of one and then decrease, which is ideal for HDR brachytherapy treatments as the distribution peak usually occurs in the tumour. The 2D anisotropy functions of both sources shown in Figure 3.3b have different trends due to the length of the ⁷⁵Se being approximately twice as long compared to the ¹⁹²Ir source. The greater length causes the ⁷⁵Se function to have the dose fall-off occur at a larger angle, allowing the deposited radiation to be more uniform along the longitudinal axis. Depending on the size and location of the tumour as well as the characteristics of the surrounding tissues, this characteristic can bring benefits to the treatment, such as giving a more conformal dose. The trade-off is that longer sources may get stuck in catheters during treatment, which is a safety concern.

Dose Rates

The dose rate of a specific source plays an important role in clinical brachytherapy treatments, as higher dose rates allow for shorter treatment times. According to the TG-43 parameters calculated in this study, for 75 Se to achieve a similar dose rate as a 10 Ci 192 Ir at a reference point of 1 cm from the source in the transverse plane in the water, the activity of the 75 Se source needs to be 2.05 ± 0.1 times larger. Notably, this finding deviates from the value of 2.3 reported in the study conducted by Weeks and Schulz (1986) [26].

The aftermentioned study by Weeks and Schulz (1986) compared the exposure rate constants of ⁷⁵Se and ¹⁹²Ir to determine the activity required for ⁷⁵Se to have a similar dose

rate as a 10 Ci ¹⁹²Ir source. The authors calculated an exposure rate constant for ⁷⁵Se to be 1.99 Rm²/hCi which aligns closely with the value derived from this study, namely 2.00 Rm²/hCi. These values were justified based on a study by Currier *et al.* (2013), which emphasized the selection of an appropriate air kerma rate constant, considering source encapsulation [78].

Several other studies, including those conducted by Shilton and Kelly (2018), as well as the U.S. Department of Health Education and Welfare, also considered the encapsulation factor and arrived at similar exposure constant values: 2.01 Rm²/hCi and 2.00 Rm²/hCi, respectively [79, 80]. It is important to consider encapsulation, as 67% unattenuated air kerma rate of ⁷⁵Se is attributable to photon energies less than 12 keV, which are attenuated by the capsule material [78]. Failure to account for this can lead to significantly higher exposure rate constants.

Hence, the discrepancy between the activity of ⁷⁵Se calculated in this study and the one calculated by Weeks and Schulz (1986) required for ⁷⁵Se to achieve an equivalent dose rate to a 10 Ci ¹⁹²Ir brachytherapy source, lies in the calculation of the exposure rate constant for ¹⁹²Ir. In this study, the calculated value was 4.08 Rm²/hCi, whereas Weeks and Shulz reported a value of 4.60 Rm²/hCi. In a literature review conducted by Glasgow and Dillon, exposure rate constant values for ¹⁹²Ir ranged from 3.948 Rcm²/hmCi (recommended in NCRP No. 41 [81]) to 4.89 Rcm²/hmCi [82]. The large difference in these values primarily arises from each investigator's utilization of different spectroscopy data. Notably, the study by Weeks and Shulz (1986) does not elaborate extensively on the calculation methodology, except for the use of 16 principle gamma rays from the ¹⁹²Ir spectrum. In contrast, this study encompasses the entire spectrum while excluding photons below 10 keV and considering the scattering and attenuation due to the source's interaction with the surrounding material,

including the capsule material and air.

3.5.2 Physical Properties

Source Activity

The expected activity of the irradiated ⁷⁵Se source was 50 mCi, which was the maximum activity permitted for handling of the source. However, after irradiation, the measured activity using the AtomLab 500 detector was 23 mCi. This discrepancy presents a concern as the close alignment between the measured and theoretically calculated activities is crucial. The observed difference introduces uncertainty when determining the irradiation time and neutron flux necessary to produce a 20 Ci ⁷⁵Se source. The activity discrepancy may be attributed to a lower quantity of ⁷⁵Se present in the source as well as the Atomlab detector used to measure the activity.

The AtomLab manual clarifies that the presented reading is, in some form, a representation of the current in the detector, which is directly proportional to the exposure rate given the fixed geometry of the unit [83]. The device is programmed with "dial values" specific to isotopes, referenced to ⁶⁰Co, with a dial value of 5.0. For ⁷⁵Se, the calculated dial value is 17.6, indicating that the exposure rate used for ⁷⁵Se would be 0.284 times that of ⁶⁰Co. The exposure rate constant of ⁶⁰Co is widely accepted as 13.0 Rcm²/hmCi [84]. Therefore, the imputed value of the exposure rate for ⁷⁵Se would be 3.96 Rcm²/hmCi. This value is higher than the exposure rate constant calculated when considering the encapsulation of the source, which is approximately 2.00 Rcm²/hmCi. This discrepancy between the theoretical and measured activities can be mainly attributed to the differences in exposure rate constants.

Radioactive Contaminants

As indicated in Table 3.1 and Table 3.2, the irradiation process generates several radioactive contaminants. It is recommended to minimize these contaminants to levels where their dosimetric contributions, within the range of clinically relevant distances near the brachytherapy source, are less than 5% of the dosimetric contributions of the primary radionuclide [64]. It was seen that through all mass arrangements of titanium and vanadium, within the specified combined mass value, which included a 10 mm titanium wire attachment to the source that would not be used clinically, the radioactive contaminants never exceeded 1% of the dosimetric contributions of ⁷⁵Se. This outcome instills confidence in the future utilization of this brachytherapy source in clinical settings, as the contaminants remain below the 5% threshold of dose contributions from the ⁷⁵Se source. However, for future investigations, it is advisable to test this source at different sites within the reactor and at different reactors, considering that the relative amounts of fast neutron activation products may vary between locations within a reactor.

3.5.3 Film Measurements

With employing a 2%/2 mm gamma index, all films successfully passed with a gamma pass rate exceeding 95%. This was achieved by incorporating a source activity correction factor and inputting individual positional correction values into the Monte Carlo simulations. Using the source activity correction factor proved necessary due to the likelihood of an inaccurate activity measurement obtained from the AtomLab 500 detector. Notably, the correction factor was within expectation as the corrected activity was greater than the original value and less than 50 mCi, which was the anticipated activity of the source.

The positional correction values compensated for various factors contributing to positional uncertainties resulting from the measurement setup using the solid water phantom. Firstly, small air gaps were inadvertently created while taping the film to the water phantom slabs and stacking them, as depicted in Figure 3.2. As the source-to-film distances increased, the cumulative effect of air gaps became more pronounced, resulting in a greater disparity between the expected and actual distances of the film. The distance correction values, obtained through iterative optimization of the gamma pass rate over a range of distances, reflected this trend. Table 3.3 presents the calculated values, revealing that shorter distance magnitudes corresponded to smaller distance correction values.

Another factor was using plastic wrap to place the source within the catheter hole, preventing any potential contamination of the water phantom slabs in direct contact with the source. This precautionary measure may have led to a slight shift in the source's precise position within the catheter channel compared to its position in the CT scans utilized in the Monte Carlo simulations taken before source irradiation. Lastly, a previous study by Aldelaijan et al. (2011) explored the impact of source position variation within different catheter sizes on film measurements. The findings indicated dosimetric errors up to 36.1% for 4F catheters and 39.8% for 6F catheters [68]. It is important to note that the study employed a setup involving a remote afterloader, whereas this current study did not utilize catheters nor a remote afterloader. Consequently, the source in this study may have experienced slight angular rotation and other positional uncertainties greater than those reported by Aldelaijan et al. (2011).

The successful comparison between film measurements and Monte Carlo simulations validated the accuracy of the dose distribution obtained from the film measurements. Utilizing a source activity correction factor and distance correction values

was necessary for the water phantom measurement setup, considering the low activity source was not amenable to manipulation using a remote afterloader. For future investigations, it is recommended to use a higher activity source controlled by a remote afterloader via catheters. Assuming the source remains intact during extended irradiation times and considering the manufacturer-provided value of 7.41 mg for the amount of ⁷⁵Se located within the source, it was determined that a 20 Ci source can be created in a typical production cycle at a high flux reactor. This production cycle would involve six weeks of irradiation time, a neutron flux of 3×10^{14} n/cm²s and a 48 hour delay before sample shipment. The determination of the higher activity source should follow a similar protocol to the established standard for clinical HDR ¹⁹²Ir sources, involving the use of an absolute dose measurement performed using a user well-type ionization chamber with a calibration traceable to a primary standard [68]. Furthermore, using a higher activity source will significantly reduce measurement times. With this benefit, it is suggested to do single film measurements to reduce air gaps that alter the expected source-to-film distance. Lastly, incorporating a remote afterloader and catheters will reduce the positional uncertainty associated with the source placement.

3.6 Conclusion

In this study, a ⁷⁵Se source with a low activity having dimensions acceptable for use in brachytherapy was manufactured. The source demonstrated excellent structural integrity without any deformations, while the presence of contaminants arising from titanium and vanadium did not pose obstacles to its potential clinical use. The high gamma pass rates observed between the film measurements and Monte Carlo simulations instilled confidence in

the accuracy and reliability of the simulations involving the ⁷⁵Se source. This confidence will be leveraged in future simulations conducted with the ⁷⁵Se source, particularly in comparative assessments of brachytherapy treatment plans involving the source alongside currently used brachytherapy sources. Utilizing ⁷⁵Se as a brachytherapy source holds significant promise; however, it is important to acknowledge that extensive further research and development are essential before its implementation in clinical settings.

3.7 Appendix A

		Element (% mass)													
Material	Density (g/cc)	Н	С	N	О	Na	Mg	Р	S	Cl	Ar	K	Ca	Si	W
Air	0.001225		0.0124	65.5268	23.1781						1.2827				
Soft Tissue	1.02	10.6	31.5	2.4	54.7	0.1		0.2	0.2	0.1		0.2			
Rectum	1.03	10.6	11.5	2.2	75.1	0.1		0.1	0.1	0.2		0.1			
Bladder (filled)	1.03	10.8	3.5	1.5	83.0	0.3		0.1	0.1	0.5		0.2			
Cortical Bone	1.92	3.4	15.5	4.2	43.5	0.1	0.2	10.3	0.3				22.5		
Silicone Rubber	1.14	0.082	0.324		0.216								0.378		
Tungsten	19.30														1

3.8 Appendix B

Item Name	Description	Reference
Code, Version	RapidBrachyMCTPS, Geant4 10.2	[19], [20]
Validation	Previously validated	[19]
Timing	30 hours, 64 cores	
Geometry	Voxelized geometry extracted from DICOM	
	CT images and DICOM RT Structure Set files.	
	CT grid interpolated to grid with voxel size: 1	
	$\times 1 \times 1 \text{ mm}^3$	
Materials	Solid water phantom with elemental	[9], [74]
	composition and mass density of tissues	
	provided in Appendix A	
Source Description	Selenium-75 Source: core diameter of 0.6 mm	[85], [73]
	and core length of 7 mm	
# Histories/Statistical	10^9 decays with Type A uncertainties of ; 0.5	
Uncertainty	% within the 1 Gy 100% isodose line.	
Statistical Methods	History-by-history method	[76]
Cross Sections	EPDL97, EEDL97, EADL97	[73], [86], [87]
Transport Parameters	PENELOPE low-energy electromagnetic	
	physics list with default transport parameters.	
	Electron Transport off. Production cut: 0.1	
	mm.	
Variance Reduction	Tracklength estimator using mass-energy	[19], [74], [87]
Technique	absorption coefficient library provided in	
	RapidBrachyMCTPS.	
Scored Quantities	Absorbed dose (collisional kerma	
	approximation) scored to medium	
Post Processing	Dose to voxels converted into dose-volume	
	parameters using RapidBrachyMCTPS.	

Chapter 4

Bridging text

The first manuscript of this thesis introduced a novel manufacturing technique for the production of a ⁷⁵Se brachytherapy source. This technique involves compounding vanadium with selenium and encapsulating the compound in a titanium capsule. The manufactured source demonstrated excellent stability, with no deformation observed after irradiation. Moreover, the analysis of radiation contaminants generated by vanadium and titanium revealed that their contribution to the overall dose remained below 1%. The characterization, using TG-43 formalism, of the source completed with the in-house Monte Carlo treatment planning software, RapidBrachyMCTPS, enabled comparison with the commonly used brachytherapy source, ¹⁹²Ir. The ⁷⁵Se source exhibited similar beneficial TG-43 qualities as ¹⁹²Ir, particularly in terms of the radial dose function and 2D anisotropy function. It was also determined that the activity of the ⁷⁵Se source only needed to be approximately twice that of the ¹⁹²Ir source to achieve a similar dose rate, which is feasible during the manufacturing process.

These results provide compelling evidence that a $^{75}\mathrm{Se}$ brachy therapy source can 4. Bridging text 50

now be manufactured using recently available methods. However, this manuscript focuses solely on establishing the feasibility of the source, and its true benefits in brachytherapy treatments have yet to be investigated. The key motivation behind the development of the ⁷⁵Se brachytherapy source lies in its lower gamma energy and longer half-life compared to ¹⁹²Ir. The hypothesis is that, with the lower gamma energy of ⁷⁵Se and the novel brachytherapy shielding techniques currently under development, significant improvements in brachytherapy treatment plans can be achieved. These improvements encompass similar treatment times, prescribed doses to the tumor and dose homogeneity, while reducing the radiation dose deposited to surrounding healthy tissues. Such reductions in radiation exposure to healthy tissues are expected to minimize future toxicities in patients and enhance their overall quality of life.

The second manuscript delves into the investigation of this hypothesis by utilizing RapidBrachyMCTPS. Initially, the study examines the differences in shielding attenuation between ⁷⁵Se and ¹⁹²Ir through simulation. Subsequently, heterogeneous patient simulations are performed to compare treatment plan metrics using both ⁷⁵Se and ¹⁹²Ir and an intensity modulated brachytherapy applicator design. These metrics include treatment times, dose homogeneity, as well as dosimetric indices of the tumor and various organs at risk. The findings from this analysis will shed further light on the potential benefits of utilizing ⁷⁵Se in conjunction with novel shielding techniques in brachytherapy treatments.

Chapter 5

Dosimetric Analysis of a Selenium-75 Brachytherapy Source

Jake Reid $^{1,4},$ Jonathan Kalinowski $^{1,4},$ Hamed Bekerat 1, John Munro III 2, Andrea Armstrong 3, Shirin A. Enger 1,4

¹Medical Physics Unit, Department of Oncology, Faculty of Medicine, McGill University, Montreal, Québec, Canada

²Burnley Technology Inc., 380 Lafayette Road, Unit 11-162, Seabrook, New Hampshire 03874, USA

 $^3\mathrm{McMaster}$ University, Nuclear Operations and Facilities, Hamilton, Ontario, Canada

⁴Lady Davis Institute for Medical Research, Jewish General Hospital, Montreal, Quebec, H3T 1E2, Canada

5.1 Abstract

Background: 75 Se ($t_{1/2} = 119$ days, $E_{\gamma,avg} = 215$ keV) is a radioisotope that is widely used in industrial gamma radiography. Its lower photon energy and longer half-life compared to 192 Ir ($t_{1/2} = 74$ days, $E_{\gamma,avg} = 360$ keV) make it a viable candidate for use as a brachytherapy source.

Purpose: This study aimed to investigate the feasibility of using a ⁷⁵Se source for brachytherapy applications and investigate its shielding properties combined with two different applicators.

Methods: An active core (0.65 mm diameter, 7 mm length, 3.7 g/cm³ packed density) of a ⁷⁵Se source was encapsulated in a titanium (4.5 g/cm³, 0.90 mm outer diameter, 0.25 mm wall thickness) capsule. The active core length was chosen to hold 23 Ci of ⁷⁵Se, providing a dose rate at a reference point 1 cm from the source in the transverse plane in water equivalent to 10 Ci of ¹⁹²Ir. All simulations were conducted using the Monte Carlo-based treatment planning system, RapidBrachyMCTPS. Dose distributions were acquired in a 30 imes 30 imes 30 cm³ water phantom for two tungsten shields: a static shield presently used in brachytherapy with a shield diameter of 8 mm and a rigid intensity-modulated brachytherapy (IMBT) shield with an emission window of 180° and a thickness of 7.5 mm. The resulting data were used to calculate the transmission factors for the different shield models and compared with simulations performed using an ¹⁹²Ir source. Both shields were tested on CT images for a rectal cancer patient treated with high dose rate brachytherapy to calculate the absorbed dose to the tumour and surrounding healthy tissue for both the 75 Se and 192 Ir sources. The treatment optimization was completed identically for both sources. For the static shield, both plans had three active catheters with dwell positions positioned with a step size of 5 mm, and for the IMBT shield, they had the dwell positions positioned along the central source channel with a step size of 5 mm and a 15° increment shield rotation. A prescription dose of $D_{90} = 10$ Gy was set.

Results: Dose distributions in a water phantom were calculated. The transmission factors displayed that 75 Se had 4.86 ± 0.12 and 5.41 ± 0.12 times better attenuation than 192 Ir for the static and rigid IMBT shields, respectively. For the calculated absorbed doses on the patient data, with all treatment plans to achieve a prescribed dose of 10 Gy to 90% of the tumour volume, the IMBT shield had the majority of the dosimetric indices improved when using the 75 Se source. The most noticeable improvements were that the D_{2cc} for the contra-lateral rectum and balloon were reduced by approximately 0.97 and 2.05 Gy, respectively, and the D_{50} of the rectum was reduced by 1.17 Gy. The treatment time was reduced by 1.2 min. For the static shield, the treatment plan for 75 Se was similar to the plan completed with 192 Ir.

Conclusions: The designed ⁷⁵Se source was superior with regards to attenuation through tungsten shields due to its lower energy while still being able to produce an equivalent dose rate to ¹⁹²Ir. This allowed for better treatment plans to be achieved when using the IMBT shield, as the treatment delivers the same absorbed dose to the tumour as ¹⁹²Ir with similar treatment times while reducing the dose to surrounding organs at risk. These results allow for justification of further analysis of this source for use in brachytherapy.

5.2 Introduction

5.2.1 High Dose Rate Brachytherapy

High dose rate (HDR) brachytherapy, especially with magnetic resonance image guidance, is one of the most effective and precise radiation delivery modalities with a major impact on gynecological, genitourinary and prostate cancers. The use of brachytherapy for the treatment of prostate cancer is an effective therapy delivered either as a monotherapy or as a boost in combination with external beam radiotherapy (EBRT) [14]. A recent multi-institutional study showed that HDR brachytherapy boost improves survival and decreases the risk of developing distant metastases compared to EBRT alone in intermediate and high-risk group prostate cancer patients [48]. A randomised trial of EBRT alone or combined with HDR brachytherapy concluded that at 12 years, there remains a significant improvement in relapse-free survival after EBRT with HDR brachytherapy boost, with both modalities being equitoxic for severe late urinary and bowel events and urethral strictures [49]. Corkum et al. (2020) investigated the long-term toxicity of HDR brachytherapy as monotherapy and found that HDR monotherapy is well tolerated with minimal impact on health-related quality of life [50]. For HDR treatment of cervical cancer, several groups have published results with image guidance showing a 17% increase in local control of large tumours and an 11% decrease in rectal bleeding [51]. In addition, combining HDR brachytherapy with EBRT compared to EBRT alone increased cancer-specific survival rates to 68.5% vs 35.4% after 5 years [52]. Intensity-modulated radiotherapy or stereotactic body radiotherapy boost resulted in inferior overall survival as compared with brachytherapy [12]. RetroEMBRACE demonstrated statistically and clinically significant local control improvement of 10% with the use of hybrid intracavitary-interstitial brachytherapy compared to intracavitary brachytherapy for large tumours [13]. For the treatment of rectal adenocarcinoma, EBRT is the best-studied form of neoadjuvant radiotherapy. However, it is associated with significant toxicities such as diarrhea, urinary symptoms, and sexual dysfunction [88, 89, 90, 91, 92]. An alternative is HDR endorectal brachytherapy, which is associated with recurrence rates comparable to those with EBRT, with fewer treatment-related toxicities and similar pre-operative outcomes with proctitis as an acute side effect [93, 94].

With the source being inserted inside or near the tumour, HDR brachytherapy offers numerous benefits for clinical treatments. However, it also has some drawbacks. These drawbacks include the invasive nature of the procedure, the requirement for substantial resources, and the radially symmetrical dose distributions produced by all sources. As a result, surrounding healthy tissue may receive higher doses compared to other treatment modalities [95].

In a study conducted by Bensaleh et al. (2009) on HDR treatments for breast cancer, it was found that brachytherapy methods treated a larger portion of the breast volume above 115% of the prescribed dose compared to 3D-CRT methods. This increased dose can lead to the production of toxicities [1]. To address this issue, static metallic shields are currently used in clinical practice to attenuate the dose. The distribution becomes radially asymmetrical by attenuating the dose, allowing for more conformal treatment plans and reducing the dose to surrounding healthy tissue [54]. Adding static shields has generally improved brachytherapy treatments, but they have the limitation of a lack of versatility in accommodating different tumour shapes and sizes [15]. Therefore, there was a need for a new application that would enable the development of optimal treatment plans tailored to each patient's specific requirements.

5.2.2 Intensity Modulated Brachytherapy

The strategy of optimizing the dose distribution using brachytherapy sources by means of tailoring the dwell positions and dwell times is limited in its ability to conform the absorbed dose to the shape of the tumour and sculpt it around the organs at risk due to the near-isotropic distribution of the individual dwells. However, similar to the revolution that occurred in EBRT with the introduction of beam intensity modulation, brachytherapy is experiencing a technological renaissance through intensity-modulated brachytherapy (IMBT) by the development of novel shielding techniques enabling collimation of brachytherapy sources that can overcome the spatial limitation of conventional sources. Several research groups have developed the next generation of HDR brachytherapy technology, including design and development of shields, rotational IMBT delivery for treatment of and rectal systems prostate, cervix, cancers [17, 22, 21, 53, 54, 15]. The importance of this research is that by incorporating metallic shields that can rotate during the treatment inside brachytherapy catheters and applicators, it will be possible to direct the radiation towards the tumour and shield the surrounding healthy tissues. By dynamically directing the radiation towards the tumour and away from healthy tissues, we can shield the normal tissues more effectively and, if needed, escalate the dose to the tumour. This may lead to increased cure rates with fewer side effects and improved patient quality of life.

Despite evidence of the significant dosimetric improvements achievable with a collimated brachytherapy source, significant practical challenges impede the clinical implementation of IMBT. Shield designs must be effective enough to attenuate the intensity of the source by several half-value layers while fitting inside existing brachytherapy catheters and applicators. This constraint limits the thickness of the shield

to the sub-millimeter range for interstitial brachytherapy and millimeters for intracavitary cases.

5.2.3 Brachytherapy Sources

 $(^{125}I$ 103 Pd, can administered by low-energy Brachytherapy be $E_{\gamma {\rm av}} < 50$ keV), intermediate energy (169Yb, $50keV > E_{\gamma {\rm av}} < 200$ keV) or high-energy $(^{192}{\rm Ir},~E_{\gamma {\rm av}}~>~200~{\rm keV})$ gamma emitting radionuclides. Low-energy photon-emitting radionuclides are used in low-dose rate (LDR) brachytherapy, with the photoelectric interaction being the dominating photon interaction process with the tissue. The dose distribution decreases rapidly with distance from the source due to strong attenuation in tissue that is not compensated by scatter. For the intermediate and high-energy brachytherapy sources, photoelectric interactions are minimal in soft tissue, Compton scattering is the dominant photon interaction. The attenuation in tissue is compensated by single/multiple-photon scatter build-up of the dose. While the dose distribution from intermediate energy sources and ¹⁹²Ir is similar, the energy of scattered photons emitted from intermediate energy sources is much lower than that of ¹⁹²Ir, with substantially lower shielding requirements for IMBT shields as well as the treatment bunkers making the technology cost-efficient and more available. Intermediate energy isotopes, including ¹⁵³Gd, $^{169}\mathrm{Yb},~^{170}\mathrm{Tm}$ and $^{57}\mathrm{Co}$ have been studied in the past for use in conventional HDR brachytherapy and IMBT [31, 36, 17, 34, 62, 18, 29, 30, 32, 33]. The scattered photons from these sources can easily be shielded by thin metal shields placed inside interstitial catheters, enabling IMBT for interstitial HDR brachytherapy. However, none of these radionuclides were suitable for clinical implementation due to limitations such as low specific activity, short half-life or high production costs.

Presently, the most common HDR brachytherapy source used in developed countries is 192 Ir ($E_{\gamma av}=360$ keV, half-life = 74 days). Due to its relatively short half-life of 74 days, 192 Ir is not used in developing countries and is replaced by 60 Co ($E_{\gamma av}=1250$ keV, half-life = 5.3 years), which has a much longer half-life as well as higher average energy than 192 Ir. Both sources are manufactured using a nuclear reactor, making the production cost-efficient. However, a new HDR source with lower energy to decrease the shielding requirements and a longer half-life than 192 Ir is desirable.

5.2.4 Selenium-75

 75 Se ($E_{\gamma av}=215$ keV, half-life = 119 days) is a radioisotope that is currently widely used in industrial gamma radiography to inspect materials, such as steel or concrete, for any defects in infrastructure [96]. 75 Se has also been studied as a potential high-energy source ($E_{av}<200$ keV) for use in HDR brachytherapy [26, 42, 24]. Many studies have investigated 75 Se with regards to the manufacturing and dosimetric properties for use in industrial gamma radiography [40, 41, 38, 39]. Still, only a few studies have been performed regarding the feasibility of 75 Se for brachytherapy applications [26, 96]. Weeks and Schulz (1986) calculated that 75 Se has an exposure rate constant 2.3 times less than 192 Ir [26]. Therefore, to achieve an equivalent dose rate at a reference point 1 cm from the source in the transverse plane in water, the 75 Se source in this study was set to have an activity that was 2.3 times greater than 192 Ir. The maximum provided 192 Ir activity clinically is about 10 Ci for HDR brachytherapy. Hence, a 23 Ci 75 Se source was desirable. The authors completed many theoretical calculations to determine the necessary aspects, such as the size of the capsule, the magnitude of neutron flux and irradiation time for developing a 23 Ci

⁷⁵Se source.

The lower photon energy emitted from ⁷⁵Se requires less shielding for brachytherapy suites. HDR brachytherapy room shielding generally requires having either 40 cm of barite concrete or 5 cm of lead [97] for ¹⁹²Ir and shielding similar to that of a teletherapy room (80 cm of concrete or 12 cm of lead [98]) for ⁶⁰Co. ⁷⁵Se only requires approximately 31 cm of barite concrete or 2.5 cm of lead for equivalent shielding [26]. This would reduce the overall costs as the construction of brachytherapy suites would require less material. Due to the reduction in shielding thickness for equivalent attenuation compared with ¹⁹²Ir, ⁷⁵Se is also of interest for IMBT. The half-value layer (HVL) in tungsten is 0.8 mm for ⁷⁵Se and 3.3 mm for ¹⁹²Ir [99]. Intracavitary applicators for treating gynecologic cancers have cavities from 5 mm (tandem for cervix applicators) up to centimeters (vaginal applicators). For rectal cancer, the size of the applicator cavity is about 15 mm. Having an HVL about a quarter of the thickness compared to the presently used source will allow for improved attenuation, potentially leading to a better-optimized treatment plan.

This study aimed to determine the potential benefits of using ⁷⁵Se compared to ¹⁹²Ir for use in brachytherapy. To accomplish this, we simulated a ⁷⁵Se source using a Monte Carlo-based treatment planning software to (1) quantitatively analyze how effective brachytherapy shields become at attenuating radiation when using ⁷⁵Se compared to ¹⁹²Ir and (2) compare optimized treatment plans that used ⁷⁵Se and ¹⁹²Ir on a single rectal cancer patient, one plan using a static shield design and the other for an IMBT shield.

5.3 Materials and Methods

In this work, the dosimetric properties of a ⁷⁵Se source were investigated, and all dosimetric comparisons are made between ⁷⁵Se and ¹⁹²Ir. The source encapsulation dimensions and materials for ⁷⁵Se are identical to the ones used in the previous manuscript, and the ¹⁹²Ir source used was the microSelectron-v2 HDR source (Nucletron, Veenendaal, Netherlands). Using a Monte Carlo-based treatment planning system, RapidBrachyMCTPS [19, 20], dose distributions in water for two rectal applicators were calculated. Two treatment plans using one fraction for one rectal cancer patient were developed using a rigid 180° IMBT shield and the cylindrical intracavitary mold applicator (ICMA) (Nucletron/Elekta; Veenendaal, the Netherlands) HDR brachytherapy applicator design for both the ⁷⁵Se and the ¹⁹²Ir sources. These optimized plans calculated the absorbed dose to the tumour and the surrounding organs at risk.

5.3.1 Monte Carlo Simulations

RapidBrachyMCTPS is a validated open-source research treatment planning system with dose optimization tools, a graphical user interface and a Monte Carlo dose calculation engine known as RapidBrachyMC [19, 20]. This software was used to simulate both a ⁷⁵Se source, the design seen in Figure 5.1, and the microSelectron-v2 HDR ¹⁹²Ir source in treatment plans using a homogeneous water phantom and a heterogeneous patient phantom. Voxellized representations of the water and patient phantom are provided to RapidBrachyMC in .egsphant format [69]. Material and densities can be assigned via a HU calibration curve or via nominal material/density assignment to contours (Appendix C). RapidBrachyMC is based on the Geant4 Monte Carlo radiation transport toolkit [70, 71, 72] where the simulation

of radioactive decay is achieved by using photon decay spectra from the Evaluated Nuclear Structure Data File [73]. All simulations were run on the Beluga cluster of the Digital Research Alliance of Canada. Since the photon energies emitted by these radioisotopes are low, it was assumed that the secondary electrons deposit their energy locally [69]. This assumption allows the dose to be approximated by collision kerma, scored using a track length estimator [74]. Utilizing multi-threading in conjunction with this approach enables a reduction in computation time. The Monte Carlo simulation parameters, seen in Appendix B, were summarized following the recommendations of TG-268 [75]. The type A uncertainty on the absorbed dose per voxel was calculated using the history-by-history method [76].

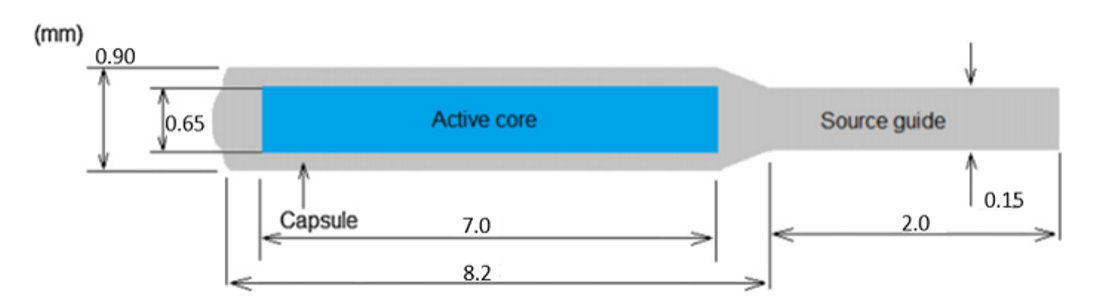


Figure 5.1: Source dimensions of the selenium source.

Simulations in Water

To quantitatively determine the difference in attenuation that brachytherapy shields achieve when using the radioisotope 75 Se compared to 192 Ir, RapidBrachyMCTPS was used to acquire dose distributions inside a uniform water phantom ($30 \times 30 \times 30 \text{ cm}^3$) using two rectal applicators: the ICMA applicator with a static shield and a rigid 180° emission window IMBT applicator designed by Thibodeau-Antonacci *et al.* [53]. These designs can be seen in Appendix A, and further analysis of these applicators can be seen in [53]. The shields were imported into RapidBrachyMCTPS in STL format, and a single dwell position

was selected halfway up the source channel with a dwell time set to 60 s. The plan was simulated with 10^8 decays with a $1 \times 1 \times 1$ mm³ scoring grid. The transmission factor (TF) was calculated to compare the shield's attenuation capability between the two sources. The equation to calculate the TF is:

$$TF = \frac{D(r = 1 \text{cm}, \theta = 90^{\circ}, \phi = 180^{\circ})}{D(r = 1 \text{cm}, \theta = 90^{\circ}, \phi = 0^{\circ})}$$
(5.1)

Where $D(r = 1 \text{ cm}, \theta = 90^{\circ}, \phi = 180^{\circ})$ is the absorbed dose 1 cm on the transverse plane from the source on the shielded side, and $D(r = 1 \text{ cm}, \theta = 90^{\circ}, \phi = 0^{\circ})$ is the absorbed dose 1 cm on the transverse plane from the source on the unshielded side.

Simulation with Patient Dataset

For the heterogeneous patient phantom simulations, one fraction of a rectal cancer patient treated at the Montreal Jewish General Hospital was used with the approval of our institutional review board. The CT images of this patient were loaded into RapidBrachyMCTPS. Organs at risk, including the pelvis, femur, bladder, and rectum, were contoured. Other contours specific to this study were also placed into the treatment plan. These include the clinical target volume (CTV), the contralateral healthy rectal wall, the balloon used to position the applicator and two cylinder contours 1 cm superior and inferior to the center of the CTV. The balloon was included as one of the objectives for the rectal IMBT applicator is to remove the need for using balloons in rectal brachytherapy. If this is achieved, the dose received to the balloon in this study would be the one received to the contralateral rectum. The two inferior and superior cylinder contours are dose spill regions used to evaluate the leakage in the inferior and superior directions. The clinical prescription dose of $D_{90} = 10$ Gy to the CTV was used.

For both 75 Se and 192 Ir simulations, the rigid 180° tungsten shield and ICMA static HDR brachytherapy shield were imported into RapidBrachyMCTPS in STL format. The applicators were placed in the voxelized patient geometry using the layered mass geometry feature for parallel worlds in Geant4 [100]. Once in place, dwell positions were inputted into appropriate source channels with a 5 mm step size between each dwell position for the 75 Se source and 192 Ir source. All dwell times were set to 1 s, 10^7 radioactive decays of the primary isotope were used, and the voxel size of $3 \times 3 \times 3$ mm³ was used. These settings were chosen to keep the computation time realistic and inexpensive. The nominal physical densities were acquired from the ICRU No. 46 [101] for all relevant organs, and the tissue elemental compositions were assigned based on the suggestions found in the AAPM TG-186 report [9]. The elemental compositions and mass densities used in the simulations can be seen in Appendix C. Each dwell position and corresponding shield rotation was simulated to get the per-dwell position dose distributions.

Once the dose distributions were acquired, the fast mixed integer optimization algorithm implemented in RapidBrachyMCTPS was used [102] to optimize a treatment plan with a CTV D_{90} dose within 1% of the prescribed dose. The dose constraints and weights for the CTV (target) and surrounding OARs were manually altered in a trial-and-error method to achieve this plan. The plan was then re-simulated to obtain a high-resolution dose map of the final plan, with a Type A uncertainty being less than 1% for voxels within the 100% isodose line. To achieve this, the simulation parameters were set to have the number of decays be 10^9 and the voxel size be set to $1 \times 1 \times 1$ mm³.

After the final simulation, dosimetric indices for both the ⁷⁵Se and ¹⁹²Ir treatments were compared to determine whether the use of a ⁷⁵Se source allowed for the dose to OARs to decrease while maintaining the prescribed dose to the CTV. More specifically, the dosimetric

indices compared were the D_{2cc} of the contralateral rectum, balloon, superior and inferior leakage contours as well as the D_{50} of these contours with the rectum, bladder, femur and pelvis. The treatment time was also determined.

5.4 Results

5.4.1 Simulations in Water

The normalization of the dose distributions was set at 1 cm from the source center on the unshielded side of the applicator. The axial views of the normalized dose maps for all water simulations can be seen in Figure 5.2. It is clearly seen that the radiation is more attenuated when using the ⁷⁵Se source compared to ¹⁹²Ir. For absorbed dose values within 1 cm from the source, the uncertainty of these simulations was all less than 0.5 %.

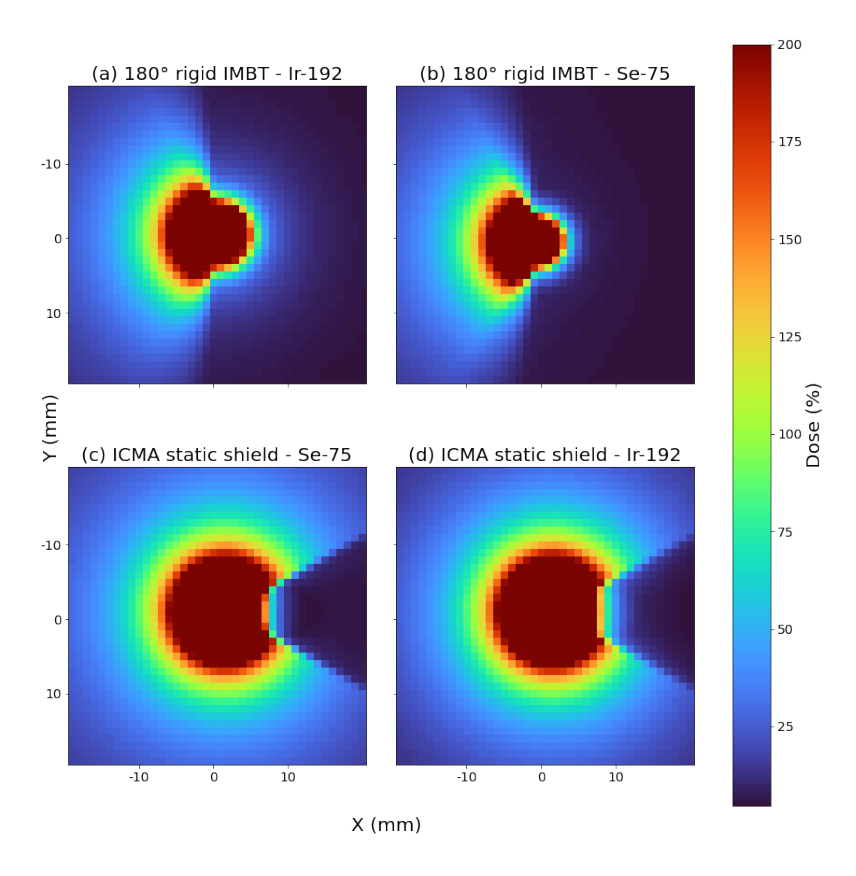


Figure 5.2: The axial dose distributions in water for both shields are used to calculate the transmission factors. a) and b) are the comparison of the rigid 180° IMBT shield for both sources, and c) and d) are the comparison of the ICMA static shield for both sources.

The TF values were calculated using Equation 5.1, seen in Table 5.1, to quantitatively analyze the attenuation of the sources with the applicators. When using the 75 Se source, the ICMA applicator and the rigid 180° IMBT applicator can reduce the absorbed dose on the shielded side by 4.86 ± 0.12 and 5.41 ± 0.12 compared to the 192 Ir source.

Table 5.1: Transmission factors for both the conventional HDR brachytherapy shield and the rigid 180° IMBT shield.

Conventional HDR Brachytherapy						
Iridium:	$20.04\% \pm 0.13\%$					
Selenium:	$4.12\% \pm 0.06\%$					
IMBT - Medical Shield						
Iridium:	$16.81\% \pm 0.13\%$					
Selenium:	$3.11\% \pm 0.06\%$					

5.4.2 Simulations in Patient

Figure 5.3 illustrates the sagittal dose distributions of the treatment plans using the ¹⁹²Ir and ⁷⁵Se sources for the IMBT shield. The selected slices in the figure effectively showcase the penetration through both the shielded and unshielded sides of the applicator. This figure shows that the radiation penetration of the ⁷⁵Se source remains within the applicator, which is desirable. In contrast, the radiation from the ¹⁹²Ir source exceeds the applicator. Figure 5.4 displays the axial dose distributions for the treatment plans using ¹⁹²Ir and ⁷⁵Se sources for the ICMA static shield. Notably, the dose distributions exhibit striking similarity. The simulations have a Type A uncertainty of less than 1% for voxels within the 100% isodose line.

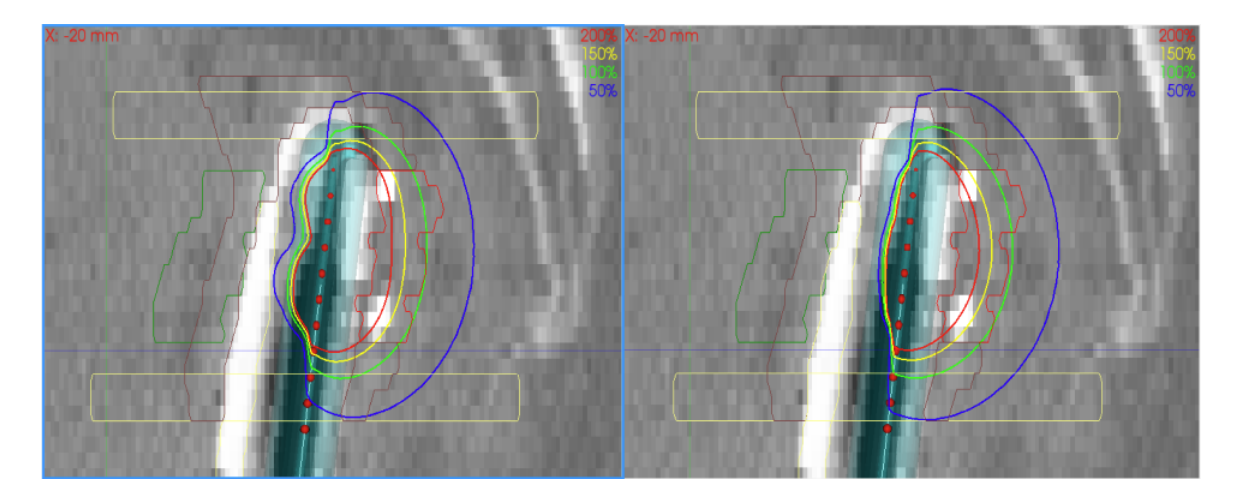


Figure 5.3: Sagittal dose distributions after final MC simulation in a heterogeneous patient phantom using the IMBT shield for the ¹⁹²Ir source (left) and ⁷⁵Se source (right). The contours displayed are the structures used to optimize the plan, and in the slices, the position of the applicator can be seen.

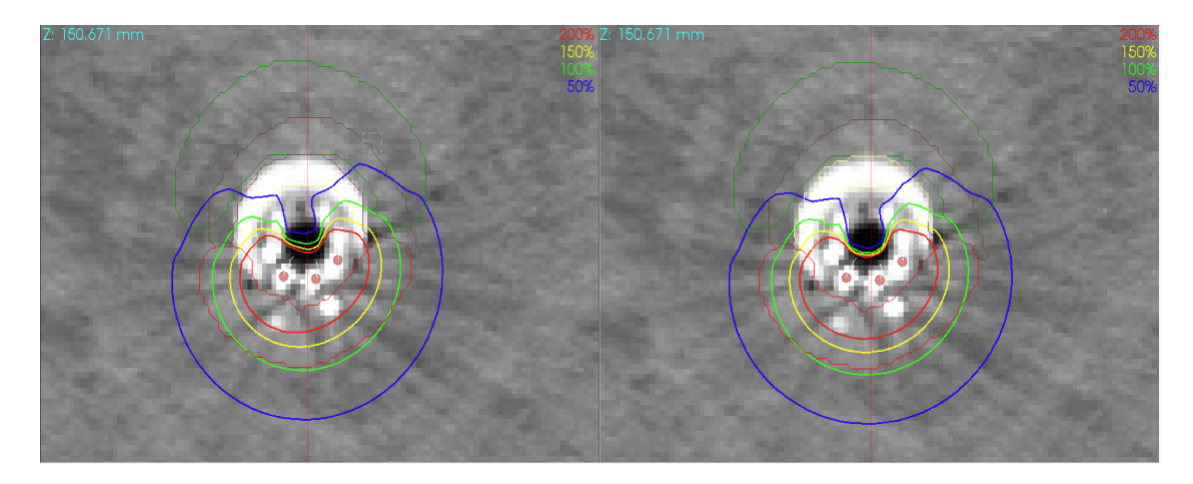


Figure 5.4: Axial dose distributions after final MC simulation in a heterogeneous patient phantom using the ICMA static shield for the ¹⁹²Ir source (left) and ⁷⁵Se source (right). The contours displayed are the structures used to optimize the plan.

The DVH metrics of the CTV and the surrounding OARs can be seen in Table 5.2. Within this table, the treatment times and the dose homogeneity indexes can also

be seen. The D_{2cc} values were used to assess the hot spots within the structures, and the D_{50} values were used to determine the dose spread in the structures. The IMBT treatment results showed that 75 Se improved the plan metrics in every aspect except for the D_{50} of the Balloon. The most noticeable improvements were that the treatment time was reduced by 1.2 min, the D_{2cc} for the contra-lateral rectum and balloon were reduced by approximately 0.97 and 2.05 Gy, respectively, and the D_{50} of the rectum was reduced by 1.17 Gy. The ICMA static shield results showed that the two sources produced similar treatment plans concerning the dosimetric indices, dose homogeneity and treatment times. The methods used to acquire the heterogeneous patient phantom dose distributions and DVH metrics can be seen in Appendix B.

Table 5.2: Plan metrics for both 75 Se and 192 Ir treatment plans using the IMBT shield. The Type A uncertainty for both plans was <1% on the 100% isodose line

	IMBT	Shield	ICMA Static Shield					
Plan Metric	Iridium-192	Selenium-75	Iridium-192	Selenium-75				
Treatment Time (min)	8.15	6.95	8.27	7.06				
$CTV D_{90\%} (Gy)$	9.94	9.94	9.93	10.01				
Contralateral D _{2cc} (Gy)	5.68	4.71	7.00	6.92				
Superior D _{2cc} (Gy)	6.52	6.09	5.34	5.56				
Inferior D _{2cc} (Gy)	6.29	6.24	5.00	5.28				
Balloon D _{2cc} (Gy)	3.30	1.25	4.76	4.98				
Contralateral D _{50%} (Gy)	1.47	0.64	2.34	2.18				
Superior D _{50%} (Gy)	1.76	1.67	1.83	1.83				
Inferior D _{50%} (Gy)	1.80	1.73	1.82	1.88				
Balloon D _{50%} (Gy)	0.30	0.31	0.90	0.86				
Rectum D _{50%} (Gy)	2.11	0.94	3.63	3.56				
Bladder D _{50%} (Gy)	0.32	0.22	0.50	0.48				
Femur D _{50%} (Gy)	0.14	0.13	0.17	0.15				
Pelvis D _{50%} (Gy)	0.33	0.29	0.45	0.43				
Dose Homogeneity Index	0.81	0.82	0.34	0.33				

The critical limitation of brachytherapy is the rotationally symmetric dose distribution provided by brachytherapy sources, delivering a high dose to the tumour but

often with poor tumour conformity due to the non-symmetrical shape of the tumours resulting in dose spillage to surrounding healthy tissues. By incorporating metallic shields that can rotate during the treatment inside brachytherapy catheters and applicators, it will be possible to direct the radiation towards the tumour and shield the surrounding healthy tissues [62]. By dynamically directing the radiation towards the tumour and away from healthy tissues, we can shield the normal tissues more effectively and, if needed, escalate the dose to the tumour [17]. Although significant dosimetric improvements are achievable with collimated brachytherapy sources, practical challenges have impeded the clinical implementation of IMBT. For example, shields must be able to attenuate the source's intensity significantly, preferably by several half-value layers, yet must be small enough to be used inside brachytherapy applicators and needles. However, a lower degree of attenuation that improves achievable dose distributions can also be beneficial [22, 21].

Due to its lower gamma energy and longer half-life than ¹⁹²Ir, in this study, ⁷⁵Se was chosen as a potential alternative to ¹⁹²Ir for the treatment of rectal cancer with IMBT. It was hypothesized that the lower mean gamma energy of ⁷⁵Se allows the shields to more effectively attenuate the dose, leading to improved treatment outcomes by reducing the dose to OARs. To test this, simulations were conducted using RapidBrachyMCTPS. A comparison of transmission factors and dosimetric indices for two rectal treatment plans demonstrated that theoretically, ⁷⁵Se is the superior source for intracavitary rectal treatments.

The transmission factor analysis showed that using the 75 Se source resulted in higher dose attenuation by the shields compared to the 192 Ir source. This outcome was expected as the HVL of 75 Se is 4.1 times shorter than 192 Ir in tungsten. However, the measured attenuation improvement factors of 4.86 ± 0.12 and 5.41 ± 0.12 for the ICMA

static HDR and IMBT shields do not perfectly align with the HVL ratio. This difference is likely attributed to differences in the measurement setup used to determine the HVL values compared to the shield simulations, taking into account factors such as the shape of the metal used and the occurrence of beam hardening phenomenon, which causes the second HVL in a beam's path to be longer than the first one. The variation in attenuation between the use of a ⁷⁵Se and ¹⁹²Ir sources were prevalent in the application of the sources for the patient simulations seen qualitatively in Figure 5.3 for the IMBT shield. However, the impact was not as significant as anticipated in the ICMA static shield treatment plans depicted in Figure 5.4.

One of the objectives of endorectal IMBT is to eliminate the use of a rectal balloon. The main uses for the rectal balloon are its effectiveness in reducing internal motion and its ability to reduce the dose received by the rectal wall. Drawbacks include the dose inhomogeneity created, which results in a lack of charged particle equilibrium and a lack of scattered radiation and added complications to the treatment such as patient discomfort [103]. The IMBT patient images show that the dose distribution for the ⁷⁵Se treatment plan does not penetrate the shield, while it does for the ¹⁹²Ir treatment plan. This lack of penetration would reduce the need for the rectal balloon as the dose received by the rectal wall would not be changed with or without the balloon when using the ⁷⁵Se source and the IMBT applicator. This observation is further supported by the dosimetric indices presented in Table 5.2, where the healthy tissues experiencing the highest dose reduction were located on the shielded side of the tungsten shield, which coincides with the location of the rectal balloon.

Both ⁷⁵Se and ¹⁹²Ir are high-energy sources, resulting in similar photon interactions, photoelectric effect and Compton scattering. Famulari *et al.* (2018) Conducted research on

the relative biological effectiveness of these two sources and found that ⁷⁵Se exhibited only a 3% higher biological effectiveness compared to the current iridium-192 sources [104]. The primary distinction between the two sources is that the mean gamma energy for ⁷⁵Se is lower than ¹⁹²Ir. Consequently, to fully leverage the benefits of a ⁷⁵Se source, effective shielding techniques are essential, as the shield will attenuate more radiation from ⁷⁵Se compared to ¹⁹²Ir.

In the case of the ICMA static shield applicator treatments, the source channels are positioned along the circumference of the applicator, which contrasts with the IMBT applicator that only has one central channel. This difference has significant implications on the effective use of the shield, resulting in escalated dose to surrounding healthy tissue, particularly to organs on the opposite side of the shield [15]. For this study's specific patient's treatment plan, three catheter channels were utilized to achieve the prescribed dose to the tumour. However, some positions were closer to the contra-lateral contour without any shielding. This treatment configuration does not allow for the advantageous lower gamma energy of ⁷⁵Se to be fully utilized. A similar outcome was also demonstrated in a previous study conducted by Shoemaker et al. (2019), where optimized treatment plans for endorectal brachytherapy using the same ICMA static shield applicator revealed similar dosimetric indices between ⁷⁵Se and ¹⁹²Ir [24]. Although the benefits of ⁷⁵Se are not evident when utilizing the currently employed ICMA static shield applicator, the ⁷⁵Se source proposed in this study still enables the development of treatment plans comparable to those using ¹⁹²Ir in terms of dose homogeneity, treatment times and the ability to achieve the prescribed dose.

This paper focuses solely on the simulation of treatment for rectal adenocarcinoma. To further demonstrate the potential benefits of using ⁷⁵Se in brachytherapy, it would be beneficial to simulate its application in other brachytherapy sites, specifically intracavitary

treatments. As mentioned earlier, the advantages of ⁷⁵Se become evident when shields are effectively employed. Effective shield usage involves considerations such as the positioning of the source relative to the shield and the shield's thickness and material.

In cases where the shield is too thin, such as in interstitial brachytherapy applications, the radiation produced by 75 Se may not be sufficiently attenuated, leading to dose distribution results similar to those obtained with 192 Ir. For such scenarios, it is recommended to use low or medium-energy radioisotopes. An example of this can be found in the study conducted by Famulari *et al.* (2019) on prostate interstitial IMBT, where shields with a thickness of 0.80 mm, made of platinum instead of tungsten, were utilized due to the constraint of catheters with a 1.45 mm diameter channel [17]. Platinum, with its higher atomic number, provides better attenuation of the radiation from the sources. However, even with the improved attenuation, 75 Se is not considered the ideal source for this application. The study simulated the system using a 169 Yb ($E_{\gamma av} = 93$ keV, half-life = 32 days) source. Nevertheless, for intracavitary applications, with adequate shield thickness and positioning techniques, such as for the IMBT applicator designed by Morcos *et al.* (2021) for cervical cancer [22], the benefits of using 75 Se as an alternative source are likely to be observed.

The ⁷⁵Se source has shown great promise as an alternative source to ¹⁹²Ir, especially in IMBT intracavitary applications. In addition to providing a conformal dose distribution to the tumour while sparing healthy surrounding tissues, brachytherapy suites would require less room shielding, as shown in the study performed by Weeks and Schulz (1986) [26]. This would reduce the implementation costs of clinics. Fewer source changes would also occur due to the longer half-life of ⁷⁵Se. Only three source changes a year for ⁷⁵Se compared to five for ¹⁹²Ir, reducing the operational costs of clinics.

5.6 Conclusion

From a dosimetric perspective, ⁷⁵Se shows significant potential as an alternative to ¹⁹²Ir for treating rectal cancer by utilizing intracavitary IMBT. It offers notable advantages in reducing the absorbed dose to organs at risk while achieving the prescribed dose to the tumour. In addition, ⁷⁵Se can produce comparable treatment plans to ¹⁹²Ir in conventional brachytherapy.

5.7 Appendix A



Figure 5.5: Intracavitary mold applicator used conventionally in HDR brachytherapy rectal treatments. Central lumen capable of holding an 8 mm tungsten shield.



Figure 5.6: Rigid 180° IMBT shield designed by Thibodeau-Antonacci *et al.* The diameter of the shield is 15 mm with 7.5 mm of tungsten shielding. The light grey part is a removable silicone rubber to enclose the central lumen.

5.8 Appendix B

Item Name	Description	Reference				
Code, Version	RapidBrachyMCTPS, Geant4 10.2					
Validation	Previously validated					
Tii	Water Phantom: 2 hours on 40 cores from a Compute Canada remote cluster					
Timing	Patient: i) 25 min and ii) 40 h on 40 cores from a Compute Canada remote cluster					
	Voxelized geometry extracted from DICOM CT images and DICOM RT Structure					
C	Set files. CT grid interpolated to grid with voxel size:					
Geometry	Water Phantom: 1 x 1 x 1 mm ³					
	Patient: i) $3 \times 3 \times 3 \text{ mm}^3$ and ii) $1 \times 1 \times 1 \text{ mm}^3$					
	Water Phantom: Homogeneous water phantom					
Materials	Patient: Heterogeneous phantom with elemental composition and mass density					
	of tissues provided in Appendix C					
Source Description	Iridium-192 Source: MicroSelectron-v2 HDR source designed by Nucletron					
	(Veenendaal, Netherlands) - core diameter of 0.6 mm and core length of 3.5 mm					
	Selenium-75 Source: core diameter of 0.6 mm and core length of 7 mm					
	Water Phantom: 10^8 photon histories with Type A uncertainties of $<1\%$					
# Histories/Statistical Uncertainty	Patient: i) 10^7 and ii) 10^9 photon histories with Type A uncertainties i) $<10\%$					
	ii) <1%					
Statistical Methods	History-by-history method	[76]				
Cross Sections	EPDL97, EEDL97, EADL97	[73], [86], [87]				
The second Discount of	PENELOPE low-energy electromagnetic physics list with default transport					
Transport Parameters	parameters. Electron Transport off. Production cut: 0.1 mm.					
Walter Dalastine Talasian	Tracklength estimator using mass-energy absorption coefficient library provided in RapidBrachyMCTPS.					
Variance Reduction Technique						
	Absorbed dose (collisional kerma approximation) scored to					
Scored Quantities	Water phantom: water					
	Patient: medium					
Post Processing	Dose to voxels converted into dose-volume parameters using RapidBrachyMCTPS.					

5.9 Appendix C

		Element (% mass)													
Material	Density (g/cc)	Н	С	N	О	Na	Mg	Р	S	Cl	Ar	K	Ca	Si	W
Air	0.001225		0.0124	65.5268	23.1781						1.2827				
Soft Tissue	1.02	10.6	31.5	2.4	54.7	0.1		0.2	0.2	0.1		0.2			
Rectum	1.03	10.6	11.5	2.2	75.1	0.1		0.1	0.1	0.2		0.1			
Bladder (filled)	1.03	10.8	3.5	1.5	83.0	0.3		0.1	0.1	0.5		0.2			
Cortical Bone	1.92	3.4	15.5	4.2	43.5	0.1	0.2	10.3	0.3				22.5		
Silicone Rubber	1.14	0.082	0.324		0.216								0.378		
Tungsten	19.30														1

Chapter 6

Discussion

Brachytherapy, both as a monotherapy and in combination with external beam radiotherapy, has emerged as a highly effective treatment modality for various cancers, including gynecological, genitourinary and prostate cancers [14, 48, 49, 50, 51, 52, 12, 13].

In this thesis, we focused on exploring ⁷⁵Se for use in brachytherapy and its integration with innovative shielding techniques, aiming to approach the ideal radiation therapy where the prescribed dose is delivered precisely to the tumour while minimizing exposure to surrounding healthy tissues.

The successful manufacturing of the ⁷⁵Se source presented in this paper was primarily facilitated by the manufactured method outlined in the patent authored by Shilton (2000) [39]. By incorporating vanadium, a stable element, with elemental selenium, the source overcame various safety concerns associated with using elemental selenium alone. These concerns encompassed the potential deformation of the source in the nuclear reactor and the creation of hazardous gas during the encapsulation process. Notably, the patent recently expired, opening up opportunities for researchers to explore the

manipulation of selenium in diverse source encapsulations, thereby enhancing various applications involving different radioisotopes. In combination with this compound, the capsule material of titanium was selected as the selenium needed to be encapsulated prior to irradiation. Although titanium and vanadium are stable elements relative to selenium, they can still undergo activation in the reactor, particularly in fast neutron fluxes. To mitigate this, it is essential to place the source in thermal neutron fluxes within the reactor. Using the thermal neutron flux at McMaster Nuclear Reactor, the total contribution of the radiation contaminants did not exceed 1% of the overall contribution of the dose, enabling it to be considered a sealed source for use in brachytherapy. If the total contribution of radiation contaminants exceeds 5% when creating higher activity sources, alternative manufacturing methods should be investigated.

While this thesis successfully manufactured a low activity ⁷⁵Se brachytherapy source, it represents only the initial step toward the clinical implementation of this design. To progress further, several important aspects need to be addressed. Firstly, a higher activity source needs to be created to meet the requirements for clinical applications. A 20 Ci ⁷⁵Se brachytherapy source would be preferable as it was determined that for a ⁷⁵Se brachytherapy source to have a similar dose rate to a 10 Ci ¹⁹²Ir source it needed 2.05 ± 0.1 times more activity. For the purpose of this study, measurements were conducted to determine the activity, radioactive contaminants, and film dosimetry of the source. An AtomLab 500 detector was used for activity measurements and a HPGe Ortec detector was used to measure the radioactive contaminants. The activity measured using the AtomLab 500 detector was approximately 40% of the theoretically calculated value. To address this concern when manufacturing a higher activity source, it is recommended to use multiple different activity detectors to allow more confidence in the measurement with one of the

measurements having a comparable procedure to the one used for clinical HDR ¹⁹²Ir sources. This process entails conducting an absolute dose measurement with a user well-type ionization chamber that has been calibrated to a primary standard, as described in the Aldelaijan *et al.* study [68]. Additionally, the radioactive contaminants of the potential higher activity source should follow the same methodology as this thesis to make sure that the overall radioactive contaminant contribution does not exceed 5% of the overall dose distribution of the ⁷⁵Se source. The source should also be irradiated in different reactors in different fluxes to get an in-depth analysis of the impact the fluxes have on the radioactive contaminants.

Due to the constraint of having to manually handle the source, the activity had to be kept low during measurements, limiting the film dosimetry setup. Manual handling of the ⁷⁵Se source without the use of catheters and a remote afterloader increases the positional uncertainties related to film dosimetry. Additionally, it was decided to take all film measurements simultaneously as with a lower activity source the time it takes to achieve an acceptable dose reading can take many hours. This method of taking all measurements simultaneously introduced air gaps created by the film and tape used, which added further positional uncertainty. With these limitations taken into consideration, as well as the underestimation of the activity, correction factors were calculated that enabled a justifiable comparison between the film and Monte Carlo dose distributions. With a higher activity source, a remote afterloader with catheters will be necessary to handle the source allowing for a reduction in positional uncertainty. Additionally, only one film measurement is recommended to be taken at a time as the measurement times for each film will take minutes instead of hours. This would remove the positional uncertainty produced by the air gaps.

For clinical implementation, preliminary tests of recommendations from regulatory guidelines need to be completed. The International Atomic Energy Agency's report on "Production techniques and quality control of sealed radioactive sources of ytterbium-169" palladium-103, iodine-125. iridium-192 and provides recommendations for quality control programs [28]. Completing these recommendations would allow the manufactured sources to pass inspection tests according to State Standard The recommended tests outlined in the report include external 24297-87 [105]. examination, temperature tests, external pressure tests, impact tests and endurance tests. External evaluation should be conducted following each of these tests to assess any deformations that may occur. Temperature tests are performed in heating and cooling devices with temperatures up to 600 °C down to -40 °C. External pressure tests require the source to withstand a pressure of 2 MPa with air. Impact tests involve using a 50 g hammer placed no less than 1 m above the source. Endurance tests require welding joints between the source and wire and between the wire and the shank, where the source needs to resist the load on rupture not less than 15H [28]. For all these tests, subjecting at least two manufactured and irradiated ⁷⁵Se brachytherapy sources are necessary to ensure consistency and reliability. Following each test, a leakage test must be performed in accordance with ISO 2919:1999E [106]. Lastly, due to the increased length of the brachytherapy source, tests must be completed to ensure the source will not get stuck in catheters during brachytherapy procedures. By adhering to these recommended regulatory tests, the quality and safety of the manufactured sources can be thoroughly assessed, providing confidence in their compliance with established standards.

Introducing metallic shields in brachytherapy catheters and applicators can potentially improve treatment outcomes by minimizing the dose received by healthy

tissues. This is particularly important due to the isotropic nature of dose distributions produced by brachytherapy sources. Despite its lower gamma energy, ⁷⁵Se is still considered a high-energy source, and the radiation it produces undergoes both photoelectric effect and Compton scattering interactions in soft tissue, similar to ¹⁹²Ir and ⁶⁰Co [2, 24, 104, 42, 21]. However, the energy of the Compton scattered photons is lower, making it easier to shield for IMBT applications, specifically for intracavitary treatments, where shields with several mm thickness are used. In contrast, interstitial IMBT brachytherapy treatments typically employ sub-milimeter shields not allowing for enough shielding for a ⁷⁵Se brachytherapy source.

Drawing from a study by Ebert *et al.* (2002), it was found that a shield transmission of less than 10% was important to achieve significant benefits from shield usage in IMBT. In the context of this thesis, this recommendation was successfully met by retrospectively employing 75 Se in conjunction with IMBT for treating rectal cancer as the transmission through the IMBT shield was $3.11 \pm 0.06\%$. Conversely, 192 Ir was found to have a transmission of $16.81 \pm 0.13\%$, exceeding the recommended 10% threshold and surpassing the 75 Se transmission by 5.4 times.

By employing ⁷⁵Se, considerable reductions in dosimetric indices for healthy tissues were achieved in the optimized treatment plan for the IMBT applicator. This improvement was particularly noteworthy for the healthy tissues located on the opposite side of the shield, with the D2cc values for the contra-lateral rectum and balloon decreasing by 0.97 Gy and 2.05 Gy, respectively, and the D50 of the rectum reducing by 1.17 Gy. The design of the applicator also played a role in these enhancements, as the source was positioned in the central channel, leading to the attenuation of the dose to the majority of the contralateral healthy tissue throughout the treatment. In contrast, the static shield technique only attenuated the dose

towards a portion of the contralateral healthy tissue, depending on the chosen catheter. These encouraging results underscore the potential of the ⁷⁵Se brachytherapy source and its compatibility with shielding techniques, ultimately improving the precision and efficacy of radiation cancer treatment.

In addition to the dosimetric advantages, using a lower gamma energy source in brachytherapy treatments can also reduce costs. Using a source with lower gamma energy necessitates less shielding for transportation and within brachytherapy suites. Weeks and Schulz (1986) conducted a study that demonstrated the potential reduction in shielding thickness when comparing a ⁷⁵Se source to a ¹⁹²Ir source, showing a 9 cm reduction for concrete shielding and a 2.5 cm reduction for lead shielding in brachytherapy suites [26]. The reductions would be even more substantial for facilities that use ⁶⁰Co, with 49 cm for concrete and 9.5 cm for lead. These findings highlight the significant cost reduction in the implementation of brachytherapy suites using ⁷⁵Se.

One of the primary reasons for the widespread use of ⁶⁰Co in developing countries, despite its high average gamma energy, is its long half-life of 5.3 years. Given the extended transportation times of brachytherapy sources to clinics in these regions, using ¹⁹²Ir is not feasible due to its short half-life. The short half-life of ¹⁹²Ir would result in limited source availability at the clinics, necessitating frequent source changes throughout the year and imposing unnecessary financial burdens. In contrast, the long half-life of ⁶⁰Co makes it an ideal choice to address this issue.

However, despite its advantages, the average gamma energy of 1.25 MeV associated with ⁶⁰Co renders novel shielding techniques developed to enhance brachytherapy treatment plans completely ineffective. On the other hand, although ⁷⁵Se has a significantly shorter half-life compared to ⁶⁰Co, its half-life of 119 days may still be sufficient to justify its use in

developing countries for improved brachytherapy treatment plans. Further investigation is required to explore the potential future applications of ⁷⁵Se in this context.

Looking ahead, further research and development in this direction hold tremendous promise for advancing the field of brachytherapy and fostering its application in real-world clinical settings. By harnessing the advantages of ⁷⁵Se and refining shielding strategies, we can strive towards more effective and targeted cancer treatments, benefiting patients and healthcare outcomes.

Chapter 7

Conclusion

This thesis presented the initial steps for manufacturing a ⁷⁵Se brachytherapy source for brachytherapy treatments. A ⁷⁵Se brachytherapy source was designed, characterized, manufactured, and measurements were taken to justify further source development. The recently available method of using a vanadium diselenide compound to manufacture the source was successful, and the hypothesized advantages that the lower gamma energy that ⁷⁵Se has in comparison to ¹⁹²Ir exceeded expectations. The radioactive contaminants resulting from including vanadium and titanium elements in the ⁷⁵Se source were found to be below the maximum recommended percentage of dose contribution to the overall dose. This effectively addresses the primary concern of using the selenium compound in combination with a titanium capsule.

An in-house Monte Carlo treatment planning software was used to characterize the source and evaluate the potential of the ⁷⁵Se source for IMBT treatment of rectal cancer compared to the commonly used brachytherapy source, ¹⁹²Ir, in optimized brachytherapy treatment plans. The treatment plan for rectal adenocarcinoma utilizing a 23 Ci ⁷⁵Se source

7. Conclusion 85

demonstrated a similar treatment time, prescribed dose to the tumour, and dose homogeneity index compared to a 10 Ci 192 Ir source. Additionally, majority of the dosimetric indices of organs at risk were reduced with the most notable reductions being the D_{2cc} for the contralateral rectum and balloon by approximately 0.97 and 2.05 Gy, respectively, and the D_{50} of the rectum by 1.17 Gy. The combination of these outcomes successfully accomplishes the objective of this thesis, which aimed to showcase the feasibility of manufacturing a 75 Se brachytherapy source and provide a compelling justification for its further development by highlighting its advantages.

For future steps to get this source to clinical implementation, a higher activity source on the order of 20 Ci needs to be manufactured and tested to ensure the source can pass all regulations set out for using brachytherapy sources in clinical treatments. By refining and expanding the capabilities of this ⁷⁵Se source, brachytherapy treatments can further be improved, allowing for a potential reduction in cost for brachytherapy treatments as well as improvement in quality of life for patients.

- [1] Saleh Bensaleh, Eva Bezak, and Martin Borg. Review of MammoSite brachytherapy: advantages, disadvantages and clinical outcomes PubMed.
- [2] Ervin B et al. Podgorsak. Radiation Oncology Physics. IAEA Vienna, 2005.
- [3] Cyrus Chargari, Eric Deutsch, Pierre Blanchard, Sebastien Gouy, Hélène Martelli, Florent Guérin, Isabelle Dumas, Alberto Bossi, Philippe Morice, Akila N. Viswanathan, and Christine Haie-Meder. Brachytherapy: An overview for clinicians. *CA: a cancer journal for clinicians*, 69(5):386–401, September 2019.
- [4] D. Chassagne, A. Dutreix, P. Almond, J. M. V. Burgers, M. Busch, and C. A. Joslin. ICRU Report 38, Dose and Volume Specification for Reporting Intracavitary Therapy in Gynecology – ICRU. Technical report.
- [5] Güler Yavaş. Dose Rate Definition in Brachytherapy. Turkish Journal of Oncology, 2019.
- [6] Subir Nag. High Dose Rate Brachytherapy: Its Clinical Applications and Treatment Guidelines. *Technology in Cancer Research & Treatment*, 3(3):269–287, 2004.

[7] R. Nath, L. L. Anderson, G. Luxton, K. A. Weaver, J. F. Williamson, and A. S. Meigooni. Dosimetry of interstitial brachytherapy sources: recommendations of the AAPM Radiation Therapy Committee Task Group No. 43. American Association of Physicists in Medicine. *Medical Physics*, 22(2):209–234, February 1995.

- [8] Mark J. Rivard, Bert M. Coursey, Larry A. DeWerd, William F. Hanson, M. Saiful Huq, Geoffrey S. Ibbott, Michael G. Mitch, Ravinder Nath, and Jeffrey F. Williamson. Update of AAPM Task Group No. 43 Report: A revised AAPM protocol for brachytherapy dose calculations. *Medical Physics*, 31(3):633–674, March 2004.
- [9] Luc Beaulieu, Asa Carlsson Tedgren, Jean-Francois Carrier, Stephen D. Davis, Firas Mourtada, Mark J. Rivard, Rowan M. Thomson, Frank Verhaegen, Todd A. Wareing, and Jeffrey F. Williamson. Report of the Task Group 186 on model-based dose calculation methods in brachytherapy beyond the TG-43 formalism: current status and recommendations for clinical implementation. Medical Physics, 39(10):6208–6236, October 2012.
- [10] G Anagnostopoulos, D Baltas, E Pantelis, P Papagiannis, and L Sakelliou. The effect of patient inhomogeneities in oesophageal 192Ir HDR brachytherapy: a Monte Carlo and analytical dosimetry study. *Physics in medicine and biology*, 49(12), June 2004. Publisher: Phys Med Biol.
- [11] G. Lymperopoulou, P. Papagiannis, A. Angelopoulos, P. Karaiskos, E. Georgiou, and D. Baltas. A dosimetric comparison of 169Yb and 192Ir for HDR brachytherapy of the breast, accounting for the effect of finite patient dimensions and tissue inhomogeneities. Medical Physics, 33(12):4583–4589, December 2006.

[12] Beant S. Gill, Jeff F. Lin, Thomas C. Krivak, Paniti Sukumvanich, Robin A. Laskey, Malcolm S. Ross, Jamie L. Lesnock, and Sushil Beriwal. National Cancer Data Base analysis of radiation therapy consolidation modality for cervical cancer: the impact of new technological advancements. *International Journal of Radiation Oncology*, *Biology, Physics*, 90(5):1083–1090, December 2014.

- [13] Kari Tanderup, Lars Ulrik Fokdal, Alina Sturdza, Christine Haie-Meder, Renaud Mazeron, Erik van Limbergen, Ina Jürgenliemk-Schulz, Primoz Petric, Peter Hoskin, Wolfgang Dörr, Søren M. Bentzen, Christian Kirisits, Jacob Christian Lindegaard, and Richard Pötter. Effect of tumor dose, volume and overall treatment time on local control after radiochemotherapy including MRI guided brachytherapy of locally advanced cervical cancer. Radiotherapy and Oncology: Journal of the European Society for Therapeutic Radiology and Oncology, 120(3):441–446, September 2016.
- [14] Magali Lecavalier-Barsoum, Farzin Khosrow-Khavar, Krum Asiev, Marija Popovic, Te Vuong, and Shirin A. Enger. Utilization of brachytherapy in Quebec, Canada. Brachytherapy, 20(6):1282–1288, 2021.
- [15] Cameron M. Callaghan, Quentin Adams, Ryan T. Flynn, Xiaodong Wu, Weiyu Xu, and Yusung Kim. Systematic Review of Intensity-Modulated Brachytherapy (IMBT): Static and Dynamic Techniques. *International Journal of Radiation Oncology, Biology, Physics*, 105(1):206–221, September 2019.
- [16] M. A. Ebert. Possibilities for intensity-modulated brachytherapy: technical limitations on the use of non-isotropic sources. *Physics in Medicine & Biology*, 47(14):2495, July 2002.

[17] Gabriel Famulari, Marie Duclos, and Shirin A. Enger. A novel 169 Yb-based dynamic-shield intensity modulated brachytherapy delivery system for prostate cancer. *Medical Physics*, 47(3):859–868, March 2020.

- [18] Gabriel Famulari, Haydee M. Linares Rosales, Justine Dupere, David C. Medich, Luc Beaulieu, and Shirin A. Enger. Monte Carlo dosimetric characterization of a new high dose rate 169 Yb brachytherapy source and independent verification using a multipoint plastic scintillator detector. *Medical Physics*, 47(9):4563–4573, September 2020.
- [19] Gabriel Famulari, Marc-André Renaud, Christopher M. Poole, Michael D. C. Evans, Jan Seuntjens, and Shirin A. Enger. RapidBrachyMCTPS: a Monte Carlo-based treatment planning system for brachytherapy applications. *Physics in Medicine and Biology*, 63(17):175007, August 2018.
- [20] Harry Glickman, Majd Antaki, Christopher Deufel, and Shirin A. Enger. RapidBrachyMCTPS 2.0: A Comprehensive and Flexible Monte Carlo-Based Treatment Planning System for Brachytherapy Applications, July 2020.
- [21] Marc Morcos and Shirin A. Enger. Monte Carlo dosimetry study of novel rotating MRI-compatible shielded tandems for intensity modulated cervix brachytherapy. *Physica medica: PM: an international journal devoted to the applications of physics to medicine and biology: official journal of the Italian Association of Biomedical Physics (AIFB)*, 71:178–184, March 2020.
- [22] Marc Morcos, Majd Antaki, Akila N. Viswanathan, and Shirin A. Enger. A novel minimally invasive dynamic-shield, intensity-modulated brachytherapy system for the treatment of cervical cancer. *Medical Physics*, 48(1):71–79, January 2021.

[23] R. A. Nout, S. Devic, T. Niazi, J. Wyse, M. Boutros, V. Pelsser, and T. Vuong. CT-based adaptive high-dose-rate endorectal brachytherapy in the preoperative treatment of locally advanced rectal cancer: Technical and practical aspects. *Brachytherapy*, 15(4):477–484, 2016.

- [24] Tristan Shoemaker, Té Vuong, Harry Glickman, Samar Kaifi, Gabriel Famulari, and Shirin A. Enger. Dosimetric Considerations for Ytterbium-169, Selenium-75, and Iridium-192 Radioisotopes in High-Dose-Rate Endorectal Brachytherapy. *International Journal of Radiation Oncology, Biology, Physics*, 105(4):875–883, November 2019.
- [25] Mahdi Bakhshabadi, Mahdi Ghorbani, Mohsen Khosroabadi, Courtney Knaup, and Ali S. Meigooni. A comparison study on various low energy sources in interstitial prostate brachytherapy. *Journal of Contemporary Brachytherapy*, 8(1):74–81, 2016.
- [26] K. J. Weeks and R. J. Schulz. Selenium-75: a potential source for use in high-activity brachytherapy irradiators. *Medical Physics*, 13(5):728–731, October 1986.
- [27] A. Mushtaq. Producing radioisotopes in power reactors. *Journal of Radioanalytical* and *Nuclear Chemistry*, 292(2):793–802, May 2012.
- [28] M. Benites, P. Chakrov, I. Cieszykowska, A. Dash, L. Falvi, H. Fan, A. R. Ghahramani, M. Haji-Saeid, H. S. Han, R. Kuznetsov, P. Mikhalevich, and H. Vera Ruiz. Production techniques and quality contril of seaed radioactive sources of palladium-103, iodine-125, iridium-192 and ytterbium-169. Technical report, International Atomic Energy Agency, June 2006.

[29] Shirin A. Enger, Michel D'Amours, and Luc Beaulieu. Modeling a Hypothetical 170Tm Source for Brachytherapy Applications. *Medical Physics*, 38(10):5307–5310, 2011. _eprint: https://aapm.onlinelibrary.wiley.com/doi/pdf/10.1118/1.3626482.

- [30] Facundo Ballester, Domingo Granero, Jose Perez-Calatayud, Jack L. M. Venselaar, and Mark J. Rivard. Study of encapsulated sources for their potential use in brachytherapy. *Medical Physics*, 37(4):1629–1637, 2010. _eprint: https://aapm.onlinelibrary.wiley.com/doi/pdf/10.1118/1.3360441.
- [31] Shirin A. Enger, Darrell R. Fisher, and Ryan T. Flynn. Gadolinium-153 as a brachytherapy isotope. *Physics in Medicine and Biology*, 58(4):957–964, February 2013.
- [32] Domingo Granero, José Pérez-Calatayud, Facundo Ballester, Adrie J. J. Bos, and Jack Venselaar. Broad-beam transmission data for new brachytherapy sources, Tm-170 and Yb-169. Radiation Protection Dosimetry, 118(1):11–15, April 2006.
- [33] Harold Perera, Jeffrey F Williamson, Zuofeng Li, Vivek Mishra, and Ali S Meigooni. Dosimetric characteristics, air-kerma strength calibration and verification of Monte Carlo simulation for a new ytterbium-169 brachytherapy source. *International Journal of Radiation Oncology*Biology*Physics*, 28(4):953–970, March 1994.
- [34] Shirin A. Enger, Hans Lundqvist, Michel D'Amours, and Luc Beaulieu. Exploring 57Co as a new isotope for brachytherapy applications. *Medical Physics*, 39(5):2342–2345, 2012. _eprint: https://aapm.onlinelibrary.wiley.com/doi/pdf/10.1118/1.3700171.

[35] L. M. Unger and D. K. Trubey. Specific gamma-ray dose constants for nuclides important to dosimetry and radiological assessment. Technical Report ORNL/RSIC-45/Rev.1, Oak Ridge National Lab., TN (USA), May 1982.

- [36] Gabriel Famulari. Production and Evaluation of Novel Brachytherapy Sources ProQuest, 2016.
- [37] Amir R Jalilian, Pejman Roushanfarzad, Mohammad Ensaf, Hossein Afarideh, Abbas Shafiee, and Hamid Rafiei. PRODUCTION OF SELENIUM-75 AND RADIOSYNTHESIS OF [75Se]-4-ETHOXYCARBONYL-5-METHYL-1,2,3-SELENADIAZOLE. page 4.
- [38] Mark Golder Shilton. Advanced, Second Generation Selenium-75 Gamma Radiography Sources, 2000.
- [39] Mark Golder Shilton and Aston Clinton. (54) GAMMA RADIATION SOURCE. 2005.
- [40] Ja. N. Gordeev, V. I. Karasev, and Ju. G. Toporov. Method for producing selenium base gamma-ray source, January 2003.
- [41] urij Evgen'evich Volchkov, Andrej Semenovich Dekopov, Nikolaj Nikolaevich Zlobin, Evgenij Mikhajlovich Kositsin, Leonid Kondrat'evich Kuznetsov, Evgenij Casil'evich Shimbarev, Vladmir Ivanovich Fedotov, and Viktor Nikolaevich Khoroshev. METHOD OF PRODUCING GAMMA-RAY SOURCES BASED ON 74Se RADIONUCLIDE FOR GAMMA-RAY FLAW DETECTION, February 2012.

[42] Gabriel Famulari, Joanne Alfieri, Marie Duclos, Té Vuong, and Shirin A. Enger. Can intermediate-energy sources lead to elevated bone doses for prostate and head & neck high-dose-rate brachytherapy? *Brachytherapy*, 19(2):255–263, 2020.

- [43] Slobodan Devic, Nada Tomic, and David Lewis. Reference radiochromic film dosimetry: Review of technical aspects. *Physica Medica*, 32(4):541–556, April 2016.
- [44] Slobodan Devic. Radiochromic film dosimetry: Past, present, and future. *Physica Medica*, 27(3):122–134, July 2011.
- [45] Sou-Tung Chiu-Tsao, Stephen Davis, Tina Pike, Larry A. DeWerd, Thomas W. Rusch, Robert R. Burnside, Manjeet Chadha, and Louis B. Harrison. Two-dimensional dosimetry for an electronic brachytherapy source using radiochromic EBT film: Determination of TG43 parameters. *Brachytherapy*, 6(2):110, April 2007.
- [46] Yi Le, E. Armour, and J. Wong. Evaluation of heterogeneity effect in intra-operative HDR (IOHDR) brachytherapy dose calculation using Monte Carlo simulation and GAFCHROMIC EBT film measurement. *Medical Physics - MED PHYS*, 34, June 2007.
- [47] M. D. C. Evans, S. Devic, and E. B. Podgorsak. High dose-rate brachytherapy source position quality assurance using radiochromic film. *Medical Dosimetry: Official Journal of the American Association of Medical Dosimetrists*, 32(1):13–15, 2007.
- [48] Marcin Miszczyk, Łukasz Magrowski, Tomasz Krzysztofiak, Rafał Stando, Wojciech Majewski, Konrad Stawiski, Oliwia Masri, Jakub Ciepał, Gabriela Depowska, Krystyna Chimiak, Gabriela Bylica, Barbara Czapla, Małgorzata Masri, Franciszek Cichur,

Iwona Jabłońska, Marta Gmerek, Zuzanna Nowicka, Piotr Wojcieszek, Jacek Sadowski, Rafał Suwiński, Paweł Rajwa, Gregor Goldner, and Matthias Moll. Brachytherapy boost improves survival and decreases risk of developing distant metastases compared to external beam radiotherapy alone in intermediate and high risk group prostate cancer patients. Radiotherapy and Oncology: Journal of the European Society for Therapeutic Radiology and Oncology, 183:109632, March 2023.

- [49] Peter J. Hoskin, Ana M. Rojas, Peter J. Ostler, Linda Bryant, and Gerry J. Lowe. Randomised trial of external-beam radiotherapy alone or with high-dose-rate brachytherapy for prostate cancer: Mature 12-year results. Radiotherapy and Oncology: Journal of the European Society for Therapeutic Radiology and Oncology, 154:214–219, January 2021.
- [50] Nicholas G. Zaorsky, Brian J. Davis, Paul L. Nguyen, Timothy N. Showalter, Peter J. Hoskin, Yasuo Yoshioka, Gerard C. Morton, and Eric M. Horwitz. Evolution of brachytherapy for prostate cancer. *Nature reviews. Urology*, 14(7):415–439, June 2017.
- [51] Linda P. Cho, Matthias Manuel, Paul Catalano, Larissa Lee, Antonio L. Damato, Robert A. Cormack, Ivan Buzurovic, Mandar Bhagwat, Desmond O'Farrell, Phillip M. Devlin, and Akila N. Viswanathan. Outcomes with volume-based dose specification in CT-planned high-dose-rate brachytherapy for stage I-II cervical carcinoma: A 10-year institutional experience. Gynecologic Oncology, 143(3):545–551, December 2016.
- [52] Johannes Karlsson, Ann-Charlotte Dreifaldt, Louise Bohr Mordhorst, and Bengt Sorbe. Differences in outcome for cervical cancer patients treated with or without brachytherapy. *Brachytherapy*, 16(1):133–140, 2017.

[53] Alana Thibodeau-Antonacci. Development of a dynamic-shielding intensity-modulated brachytherapy applicator for the treatment of rectal cancer.

- [54] William Y. Song and Shirin A. Enger. Commentary on Systematic Review of Intensity Modulated Brachytherapy (IMBT): Static and Dynamic Techniques. *International Journal of Radiation Oncology, Biology, Physics*, 105(3):493–494, November 2019. Publisher: Elsevier.
- [55] Quentin Adams, Karolyn M. Hopfensperger, Yusung Kim, Xiaodong Wu, Weiyu Xu, Hemant Shukla, James McGee, Joseph M. Caster, and Ryan T. Flynn. Effectiveness of Rotating Shield Brachytherapy for Prostate Cancer Dose Escalation and Urethral Sparing. International journal of radiation oncology, biology, physics, 102(5):1543–1550, December 2018.
- [56] Quentin E. Adams, Jinghzu Xu, Elizabeth K. Breitbach, Xing Li, Shirin A. Enger, William R. Rockey, Yusung Kim, Xiaodong Wu, and Ryan T. Flynn. Interstitial rotating shield brachytherapy for prostate cancer. *Medical Physics*, 41(5):051703, May 2014.
- [57] Myung Cho, Xiaodong Wu, Hossein Dadkhah, Jirong Yi, Ryan T. Flynn, Yusung Kim, and Weiyu Xu. Fast dose optimization for rotating shield brachytherapy. *Medical Physics*, 44(10):5384–5392, October 2017.
- [58] Hossein Dadkhah, Karolyn M. Hopfensperger, Yusung Kim, Xiaodong Wu, and Ryan T. Flynn. Multisource Rotating Shield Brachytherapy Apparatus for Prostate Cancer. *International Journal of Radiation Oncology, Biology, Physics*, 99(3):719–728, November 2017.

[59] Hossein Dadkhah, Yusung Kim, Xiaodong Wu, and Ryan T. Flynn. Multihelix rotating shield brachytherapy for cervical cancer. *Medical Physics*, 42(11):6579–6588, November 2015.

- [60] M. A. Ebert. Potential dose-conformity advantages with multi-source intensity-modulated brachytherapy (IMBT). Australasian Physical & Engineering Sciences in Medicine, 29(2):165–171, June 2006.
- [61] Mahdi Ghorbani, Benyamin Khajetash, Najmeh Ghatei, Mohammad Mehrpouyan, Ali S. Meigooni, and Ramin Shahraini. Determination of dosimetric parameters for shielded 153Gd source in prostate cancer brachytherapy. Radiology and Oncology, 51(1):101–112, February 2017.
- [62] Marc Morcos, Akila N. Viswanathan, and Shirin A. Enger. On the impact of absorbed dose specification, tissue heterogeneities, and applicator heterogeneities on Monte Carlo-based dosimetry of Ir-192, Se-75, and Yb-169 in conventional and intensity-modulated brachytherapy for the treatment of cervical cancer. *Medical Physics*, 48(5):2604–2613, May 2021.
- [63] C. Ballaux. Gamma radiography with 75Se sources: consequences of a violent fire. Health Physics, 78(3):311–315, March 2000.
- [64] Ravinder Nath, Mark J. Rivard, Larry A. DeWerd, William A. Dezarn, H. Thompson Heaton II, Geoffrey S. Ibbott, Ali S. Meigooni, Zoubir Ouhib, Thomas W. Rusch, Frank-André Siebert, and Jack L. M. Venselaar. Guidelines by the AAPM and GEC-ESTRO on the use of innovative brachytherapy devices and applications:

Report of Task Group 167. *Medical Physics*, 43(6Part1):3178–3205, 2016. Leprint: https://onlinelibrary.wiley.com/doi/pdf/10.1118/1.4951734.

- [65] Jonathan Kalinowski, Gabriel Famulari, and Shirin A. Enger. PP24 Presentation Time: 4:10 PM: RapidBrachyTG43: A Geant4-Based TG-43 Parameter Calculation Engine for Brachytherapy Applications. *Brachytherapy*, 20(3):S21–S22, May 2021. Publisher: Elsevier.
- [66] Livechart Table of Nuclides Nuclear structure and decay data.
- [67] David Lewis, Andre Micke, Xiang Yu, and Maria F. Chan. An efficient protocol for radiochromic film dosimetry combining calibration and measurement in a single scan. *Medical Physics*, 39(10):6339–6350, 2012. _eprint: https://onlinelibrary.wiley.com/doi/pdf/10.1118/1.4754797.
- [68] Saad Mohammed, Aldelaijan, Huriyyah Nada Tomic. Li-Heng Liang, Francois DeBlois, Arman Sarfehnia, Wamied Abdel-Rahman, Jan Seuntjens, and Slobodan Devic. Radiochromic film dosimetry of HDR 192Ir source radiation fields. Medical Physics, 38(11):6074-6083, 2011. _eprint: https://onlinelibrary.wiley.com/doi/pdf/10.1118/1.3651482.
- [69] R. E. P. Taylor and D. W. O. Rogers. EGSnrc Monte Carlo calculated dosimetry parameters for 192Ir and 169Yb brachytherapy sources. *Medical Physics*, 35(11):4933– 4944, November 2008.
- [70] S. Agostinelli, J. Allison, K. Amako, J. Apostolakis, H. Araujo, P. Arce, M. Asai, D. Axen, S. Banerjee, G. Barrand, F. Behner, L. Bellagamba, J. Boudreau,

L. Broglia, A. Brunengo, H. Burkhardt, S. Chauvie, J. Chuma, R. Chytracek, G. Cooperman, G. Cosmo, P. Degtyarenko, A. Dell'Acqua, G. Depaola, D. Dietrich, R. Enami, A. Feliciello, C. Ferguson, H. Fesefeldt, G. Folger, F. Foppiano, A. Forti, S. Garelli, S. Giani, R. Giannitrapani, D. Gibin, J. J. Gomez Cadenas, I. Gonzalez, G. Gracia Abril, G. Greeniaus, W. Greiner, V. Grichine, A. Grossheim, S. Guatelli, P. Gumplinger, R. Hamatsu, K. Hashimoto, H. Hasui, A. Heikkinen, A. Howard, V. Ivanchenko, A. Johnson, F. W. Jones, J. Kallenbach, N. Kanaya, M. Kawabata, Y. Kawabata, M. Kawaguti, S. Kelner, P. Kent, A. Kimura, T. Kodama, R. Kokoulin, M. Kossov, H. Kurashige, E. Lamanna, T. Lampen, V. Lara, V. Lefebure, F. Lei, M. Liendl, W. Lockman, F. Longo, S. Magni, M. Maire, E. Medernach, K. Minamimoto, P. Mora de Freitas, Y. Morita, K. Murakami, M. Nagamatu, R. Nartallo, P. Nieminen, T. Nishimura, K. Ohtsubo, M. Okamura, S. O'Neale, Y. Oohata, K. Paech, J. Perl, A. Pfeiffer, M. G. Pia, F. Ranjard, A. Rybin, S. Sadilov, E. Di Salvo, G. Santin, T. Sasaki, N. Savvas, Y. Sawada, S. Scherer, S. Sei, V. Sirotenko, D. Smith, N. Starkov, H. Stoecker, J. Sulkimo, M. Takahata, S. Tanaka, E. Tcherniaev, E. Safai Tehrani, M. Tropeano, P. Truscott, H. Uno, L. Urban, P. Urban, M. Verderi, A. Walkden, W. Wander, H. Weber, J. P. Wellisch, T. Wenaus, D. C. Williams, D. Wright, T. Yamada, H. Yoshida, and D. Zschiesche. GEANT4-a simulation toolkit. Nuclear Instruments and Methods in Physics Research. Section A, Accelerators, Spectrometers, Detectors and Associated Equipment, 506, July 2003.

[71] J. Allison, K. Amako, J. Apostolakis, H. Araujo, P. Arce Dubois, M. Asai, G. Barrand, R. Capra, S. Chauvie, R. Chytracek, G.A.P. Cirrone, G. Cooperman, G. Cosmo, G. Cuttone, G.G. Daquino, M. Donszelmann, M. Dressel, G. Folger, F. Foppiano,

J. Generowicz, V. Grichine, S. Guatelli, P. Gumplinger, A. Heikkinen, I. Hrivnacova, A. Howard, S. Incerti, V. Ivanchenko, T. Johnson, F. Jones, T. Koi, R. Kokoulin, M. Kossov, H. Kurashige, V. Lara, S. Larsson, F. Lei, O. Link, F. Longo, M. Maire, A. Mantero, B. Mascialino, I. McLaren, P. Mendez Lorenzo, K. Minamimoto, K. Murakami, P. Nieminen, L. Pandola, S. Parlati, L. Peralta, J. Perl, A. Pfeiffer, M.G. Pia, A. Ribon, P. Rodrigues, G. Russo, S. Sadilov, G. Santin, T. Sasaki, D. Smith, N. Starkov, S. Tanaka, E. Tcherniaev, B. Tome, A. Trindade, P. Truscott, L. Urban, M. Verderi, A. Walkden, J.P. Wellisch, D.C. Williams, D. Wright, and H. Yoshida. Geant4 developments and applications. *IEEE Transactions on Nuclear Science*, 53(1):270–278, February 2006.

[72] J. Allison, K. Amako, J. Apostolakis, P. Arce, M. Asai, T. Aso, E. Bagli, A. Bagulya,
S. Banerjee, G. Barrand, B. R. Beck, A. G. Bogdanov, D. Brandt, J. M. C.
Brown, H. Burkhardt, Ph. Canal, D. Cano-Ott, S. Chauvie, K. Cho, G. A. P.
Cirrone, G. Cooperman, M. A. Cortés-Giraldo, G. Cosmo, G. Cuttone, G. Depaola,
L. Desorgher, X. Dong, A. Dotti, V. D. Elvira, G. Folger, Z. Francis, A. Galoyan,
L. Garnier, M. Gayer, K. L. Genser, V. M. Grichine, S. Guatelli, P. Guèye,
P. Gumplinger, A. S. Howard, I. Hřivnáčová, S. Hwang, S. Incerti, A. Ivanchenko, V. N.
Ivanchenko, F. W. Jones, S. Y. Jun, P. Kaitaniemi, N. Karakatsanis, M. Karamitros,
M. Kelsey, A. Kimura, T. Koi, H. Kurashige, A. Lechner, S. B. Lee, F. Longo,
M. Maire, D. Mancusi, A. Mantero, E. Mendoza, B. Morgan, K. Murakami, T. Nikitina,
L. Pandola, P. Paprocki, J. Perl, I. Petrović, M. G. Pia, W. Pokorski, J. M. Quesada,
M. Raine, M. A. Reis, A. Ribon, A. Ristić Fira, F. Romano, G. Russo, G. Santin,
T. Sasaki, D. Sawkey, J. I. Shin, I. I. Strakovsky, A. Taborda, S. Tanaka, B. Tomé,

T. Toshito, H. N. Tran, P. R. Truscott, L. Urban, V. Uzhinsky, J. M. Verbeke, M. Verderi, B. L. Wendt, H. Wenzel, D. H. Wright, D. M. Wright, T. Yamashita, J. Yarba, and H. Yoshida. Recent developments in Geant4. Nuclear Instruments and Methods in Physics Research Section A: Accelerators, Spectrometers, Detectors and Associated Equipment, 835:186–225, November 2016.

- [73] J.K. Tuli. Evaluated nuclear structure data file. Nuclear Instruments and Methods in Physics Research Section A: Accelerators, Spectrometers, Detectors and Associated Equipment, 369(2-3):506-510, February 1996.
- [74] J. F. Williamson. Monte Carlo evaluation of kerma at a point for photon transport problems. *Medical Physics*, 14(4):567–576, 1987.
- [75] Ioannis Sechopoulos, D. W. O. Rogers, Magdalena Bazalova-Carter, Wesley E. Bolch, Emily C. Heath, Michael F. McNitt-Gray, Josep Sempau, and Jeffrey F. Williamson. RECORDS: improved Reporting of montE CarlO RaDiation transport Studies: Report of the AAPM Research Committee Task Group 268. Medical Physics, 45(1):e1-e5, January 2018.
- [76] B. R. B. Walters, I. Kawrakow, and D. W. O. Rogers. History by history statistical estimators in the BEAM code system. *Medical Physics*, 29(12):2745–2752, December 2002.
- [77] Titanium | Element, Meaning, Symbol, Density, Properties, Uses, & Facts | Britannica.
- [78] Blake H Currier, John J. Munro, and David C. Medich. Selection of an appropriate air kerma rate constant for 75Se sources. *Health Physics*, 104(5):511–516, May 2013.

[79] M G Shilton. Safety Performance of Se-75 Radiography Sources. *QSA Global Inc.*, 2018.

- [80] RADIOLOGICAL HEALTH HANDBOOK. Technical Report PHS-PUBL.-2016, Public Health Service, Rockville, Md., January 1970.
- [81] MMD William, IM Grotenhuis, A Raventos, and RJ Shalek. Report No. 041 Specification of Gamma-Ray Brachytherapy Sources (1974) - NCRP | Bethesda, MD, July 2018.
- [82] G. P. Glasgow and L. T. Dillman. Specific gamma-ray constant and exposure rate constant of 192Ir. *Medical Physics*, 6(1):49–52, 1979.
- [83] AtomLab 500 Dose Calibrator. Operation and service manual, BIODEX, New York, 2016.
- [84] Daryoush Khoramian and Valiallah Saba. Calculation of Exposure Rate Constant for 60 Co, 22 Na and 111 In Sources with FLUKA Monte Carlo Code. *Journal of Paramedical Sciences (JPS)*, 8:18–21, July 2017.
- [85] Facundo Ballester, Åsa Carlsson Tedgren, Domingo Granero, Annette Haworth, Firas Mourtada, Gabriel Paiva Fonseca, Kyveli Zourari, Panagiotis Papagiannis, Mark J. Rivard, Frank-André Siebert, Ron S. Sloboda, Ryan L. Smith, Rowan M. Thomson, Frank Verhaegen, Javier Vijande, Yunzhi Ma, and Luc Beaulieu. A generic high-dose rate (192)Ir brachytherapy source for evaluation of model-based dose calculations beyond the TG-43 formalism. *Medical Physics*, 42(6):3048–3061, June 2015.

[86] D. E. Cullen, J. H. Hubbell, and L. Kissel. EPDL97: the evaluated photo data library '97 version. Technical Report UCRL-50400-Vol.6-Rev.5, Lawrence Livermore National Lab. (LLNL), Livermore, CA (United States), September 1997.

- [87] S. T. Perkins, D. E. Cullen, and S. M. Seltzer. Tables and graphs of electron-interaction cross sections from 10 eV to 100 GeV derived from the LLNL Evaluated Electron Data Library (EEDL), Z = 1–100. Technical Report UCRL-50400-Vol.31, Lawrence Livermore National Lab., CA (United States), November 1991.
- [88] Robert Díaz Beveridge, Dilara Akhoundova, Gema Bruixola, and Jorge Aparicio. Controversies in the multimodality management of locally advanced rectal cancer. Medical Oncology (Northwood, London, England), 34(6):102, June 2017.
- [89] Mark W. Onaitis, Robert B. Noone, Matthew Hartwig, Herbert Hurwitz, Michael Morse, Paul Jowell, Kevin McGrath, Catherine Lee, Mitchell S. Anscher, Bryan Clary, Christopher Mantyh, Theodore N. Pappas, Kirk Ludwig, Hilliard F. Seigler, and Douglas S. Tyler. Neoadjuvant Chemoradiation for Rectal Cancer: Analysis of Clinical Outcomes From a 13-Year Institutional Experience. Annals of Surgery, 233(6):778–785, June 2001.
- [90] Aparna Kalyan, Shaina Rozelle, and Al Benson. Neoadjuvant treatment of rectal cancer: where are we now? Gastroenterology Report, 4(3):206–209, August 2016.
- [91] C. Gani, P. Bonomo, K. Zwirner, C. Schroeder, A. Menegakis, C. Rödel, and D. Zips. Organ preservation in rectal cancer - Challenges and future strategies. *Clinical and Translational Radiation Oncology*, 3:9–15, April 2017.

[92] Claire O'Gorman, Suzanne Denieffe, and Martina Gooney. Literature review: preoperative radiotherapy and rectal cancer - impact on acute symptom presentation and quality of life. *Journal of Clinical Nursing*, 23(3-4):333–351, February 2014.

- [93] Té Vuong, Slobodan Devic, Belal Moftah, Michael Evans, and Ervin B. Podgorsak. High-dose-rate endorectal brachytherapy in the treatment of locally advanced rectal carcinoma: technical aspects. *Brachytherapy*, 4(3):230–235, 2005.
- [94] Té Vuong and Slobodan Devic. High-dose-rate pre-operative endorectal brachytherapy for patients with rectal cancer. *Journal of Contemporary Brachytherapy*, 7(2):183–188, April 2015.
- [95] Robyn Banerjee and Mitchell Kamrava. Brachytherapy in the treatment of cervical cancer: a review. *International Journal of Women's Health*, 6:555–564, May 2014.
- [96] A. V. Belousov, A. A. Belianov, G. A. Krusanov, and A. P. Chernyaev. Simulation of 75Se Encapsulated Sources for Their Potential Use in Brachytherapy. *Moscow University Physics Bulletin*, 73(3):339–341, May 2018.
- [97] P. Papagiannis, D. Baltas, D. Granero, J. Pérez-Calatayud, J. Gimeno, F. Ballester, and J. L. M. Venselaar. Radiation transmission data for radionuclides and materials relevant to brachytherapy facility shielding. *Medical Physics*, 35(11):4898–4906, 2008. Leprint: https://aapm.onlinelibrary.wiley.com/doi/pdf/10.1118/1.2986153.
- [98] A. Hagemann, P. Legoux, H.M. Morgan, M. Oresegun, E. Reber, and R.K. Wu. Radiation Protection in the Design of Radiotherapy Facilities, September 2006.
- [99] QSA 880 Series User Manual. Technical report, QSA Global Inc., 2022.

[100] Shirin A. Enger, Guillaume Landry, Michel D'Amours, Frank Verhaegen, Luc Beaulieu, Makoto Asai, and Joseph Perl. Layered mass geometry: a novel technique to overlay seeds and applicators onto patient geometry in Geant4 brachytherapy simulations. *Physics in Medicine and Biology*, 57(19):6269–6277, October 2012.

- [101] M Bethesda. Photon, electron, proton and neutron interaction data for body tissues. Technical Report ICRU-46, International Commission on Radiation Units and Measurements, Bethesda, MD (United States), February 1992.
- [102] Majd Antaki, Christopher L. Deufel, and Shirin A. Enger. Fast mixed integer optimization (FMIO) for high dose rate brachytherapy. *Physics in Medicine & Biology*, 65(21):215005, November 2020. Publisher: IOP Publishing.
- [103] Shiv P. Srivastava, Indra J. Das, Arvind Kumar, Peter A. S. Johnstone, and Chee-Wai Cheng. Impact of rectal balloon-filling materials on the dosimetry of prostate and organs at risk in photon beam therapy. *Journal of Applied Clinical Medical Physics*, 14(1):81–91, January 2013.
- [104] Gabriel Famulari, Piotr Pater, and Shirin A. Enger. Microdosimetric Evaluation of Current and Alternative Brachytherapy Sources-A Geant4-DNA Simulation Study. International Journal of Radiation Oncology, Biology, Physics, 100(1):270–277, January 2018.
- [105] Goods inwards tests. Basic Principles. GOST 24297-87. Technical report, State Standardization Committee, Moscow, 1987.
- [106] Radiation protection-Sealed radioactive sources-Leakage test methods. Technical report, 1992.